Effect of Salinity on the Warm Water-Based Processing of Mineable Oil Sands

by

Tong Chen

A thesis submitted in partial fulfillment of the requirements for the degree of

Master of Science
in
Chemical Engineering

Department of Chemical and Materials Engineering
University of Alberta

Abstract

Due to the extensive usage of caustics and increased level of water recycling, the inevitable increase in salinity of recycle process water is a growing challenge in the current water-based bitumen extraction process. The present work concerns about how salinity affects bitumen recovery from various oil sands ores. Laboratory flotation results demonstrate that the decrease in bitumen recovery and froth quality by increasing the salinity of process water at pH 8.5 was ore-dependent. Increasing the salinity of process water caused a dramatic decrease in ore processability for the low-grade processing ores. In contrast, the increase in salinity up to 4000 ppm NaCl concentration in the process water showed a negligible effect on the processability of high-grade processing ores. Interestingly, the use of caustic to increase the pH of process water to 11.2 could not alleviate, but increase, the negative effect of salinity on the processability of low-grade ores.

Systematic study was conducted to understand the significant effect of increasing salinity on bitumen recovery from poor processing ores. Using our refined in-situ bitumen liberation flow visualization cell, the salt addition was found to decrease the degree of bitumen liberation (DBL) from low-grade ores. At higher pH, the negative effect of salinity on the DBL was more evident. The zeta potential measurement revealed that the incremental zeta potential of fines and bitumen become less negative as the increase of salt concentration. The result from the induction time measurement also showed that increasing sodium concentration inhibits bitumen and bubble

attachment in the presence of fines. The detrimental effect of salinity on bitumen aeration was more profound at higher pH of the process water. The results from this study aided to develop strategies of blending low-grade ore with high-grade ore, to minimize the negative impact of increased recycle water salinity on bitumen extraction.

Acknowledgement

I would like to thank Dr. Zhenghe Xu and Dr Feng Lin, for their guidance and support upon me throughout the course of my research project.

I would also like to express my thanks to Mr. Jim Skwarok, Ms. Jie Ru and Ms. Lisa Carreiro for all of their endless help. I would also like to thank Bauyrzhan Kerimkulovich Primkulov (a graduate student from our group) who assisted in conducting the contact angle measurements of the results reported in this thesis. Additional, I would like to extend my gratitude to the entire Oil Sands Extraction research group for their valuable ideas and discussions.

Last but not the least, I like to acknowledge the financial support from the Natural Sciences and Engineering Research Council of Canada (NSERC) under the Industrial Research Chair Program in Oil Sands Engineering and the sample (ore, process water, bitumen and clay fines) provided by Syncrude Canada Ltd. and Teck Corporation.

Table of Contents

Chapter 1: Introduction 1
1.1 Oil Sands 1
1.2 Bitumen Production 2
1.2.1 Hot/Warm Water-Based Bitumen Extraction 3
1.3 Tailings and Water Treatment 5
1.4 Problem Identification: Water Salinity 7
1.5 Thesis Objectives 9
1.6 Thesis Outline 9
Chapter 2: Literature Review 11
2.1 Colloids 11
2.2 Electrical Double Layer and DLVO Theory 12
2.3 Fundamentals of Bitumen Extraction 15
2.3.1 Bitumen Liberation 16
2.3.2 Bitumen Aeration 18
2.3.3 Other Relevant Studies 23
Chapter 3: Materials and Methods 24
3.1 Oil Sands Characterization 24
3.2 Chemistry of Process Water 25
3.3 Mineralogy of Clay Fines 26
3.4 Experimental Methods 27
3.4.1 Bitumen Flotation 27
3.4.2 Dean Stark Analysis 28
3.4.3 Bitumen Liberation 29
3.4.4 Contact Angle Measurement 32
3.4.5 Induction Time Measurement 34
3.4.6 Zeta-potential Measurement 37
Chapter 4: Results and Discussion 38
4.1 Effect of Salinity on Bitumen Extraction 38
4.2 Working Mechanism of Salinity Impact 41
4.2.1 Bitumen Liberation 42
4.2.2 Contact Angle Measurement 43
4.2.3 Induction Time of Bitumen Aeration 44
4.2.4 Zeta Potentials of Suspended Fines and Bitumen 47
4.3 Remediation via Caustic Addition: a Strategy of Failure 49
4.3.1 Effect of salinity on bitumen flotation at increased pH 50
4.3.2 Effect of salinity on bitumen liberation at more alkaline pH 52
4.3.3 Effect of salinity on bitumen recession at more alkaline pH 54
4.3.4 Effect of salinity on bitumen aeration at more alkaline pH 55
4.3.5 Effect of salinity on zeta-potential at more alkaline pH 56
4.3.6 Discussion 57
4.4 Positive Strategy — Blending of Different-Grade Ores 59
Chapter 5: Conclusions 61

List of Tables

Table 3.1: Composition (wt%) of oil sands ores. 24
Table 3.2: Average composition of process water 26
Table 3.3: Clay mineralogy for the fines used in induction time measurement. 26

List of Figures

Figure 1.1: The microscopic structure of Athabasca oil sands proposed by Takamura. 1

Figure 1.2: Generalized scheme for oil sands processing using hot water based extraction process. 4

Figure 1.3: Scheme of Tailings Pond.....6

Figure 2.1: Schematics of electrical double layer based on Stern model. 14

Figure 2.2: The profile of the three potentials in the Stern model. 14

Figure 2.3: Gibbs free energy (normalized by k_BT) of interaction versus distance for two identical spherical particles of R = 100 nm radius in water, containing different concentrations of monovalent salt. The calculation is based on DLVO theory. The Hamaker constant $A_H = 7\times10^{-21}$ J, surface potential ψ_0 = 30 mV. The insert shows the weak attractive interaction (secondary energy minimum) at very large distances. 15

Figure 2.4: Schematic of bitumen liberation from a sand grain.....16

Figure 2.5: Aqueous contact angle of bitumen on a sand grain. 17

Figure 2.6: Schematics of (a) bitumen-air attachment and (b) air engulfment 19

Figure 2.7: Aqueous contact angle of air bubble on bitumen surface.....21

Figure 2.8: Induction time of air-bitumen attachment as a function of temperature: (a) in clear process water and (b) in process water containing 0.5 wt% fines. 22

Figure 2.9: Schematics showing the impact of calcium on silica-bitumen interactions. Negatively charged for (a) bitumen and (b) silica surfaces in alkaline solution; (c) calcium acts as a binder between the silica and bitumen surfaces. 22

Figure 3.1: Solid size distribution of three ores. 25

Figure 3.2: Scheme for the Denver flotation cell.....28

Figure 3.3: Bitumen liberation experimental setup. 31

Figure 3.4: Procedure of determining the degree of bitumen liberation (DBL). 31

Figure 3.5: Examples showing bitumen liberation image analysis. 32

Figure 3.6: Typical images showing bitumen micro-droplet relaxation. 33

Figure 3.7: Schematics of determining contact angle using a shape fitting method. 34

Figure 3.8: The procedure of preparing the sample of bitumen coated with fines. 35

Figure 3.9: Schematics of induction timer setup. 37

Figure 4.1: Effect of salinity on bitumen recovery from the three ores: (a) primary and (b) overall flotation 39

Figure 4.2: Effect of salinity on the mass of bitumen, solids and water in the primary froth: (a) Sun08, (b) MA (middle) and (c) AE13, respectively. 40

Figure 4.3: Effect of salinity on the mass of bitumen, solids and water in the overall froth: (a) Sun08, (b) MA, and (c) AE13, respectively. 40

Figure 4.4: Effect of salinity on bitumen/solids ratio: (a) primary froth and (b) overall froth. 41

Figure 4.5: Effect of salinity on the degree of bitumen liberation (DBL) from the three ores at pH 8.5: (a) Sun08, (b) MA, and (c) AE13, respectively.. 43

Figure 4.6: Effect of salinity on the dynamic and static contact angles of bitumen recession from a glass microsphere in simulated process water at pH 8.5.....44

Figure 4.7: Effect of salinity on probability of air bubble attachment with: (a) bare bitumen and (b) fines-coated bitumen. 46
Figure 4.8: Effect of clay fines on bitumen and air bubble attachment. 47
Figure 4.9: Illustration of bitumen and air bubble attachment (a) without fines and (b) with fines 47
Figure 4.10: Zeta potentials of suspended fines (taken from the froth) and VDU bitumen in clear tailings water at pH = 8.5. 48
Figure 4.11: Effect of salinity on bitumen (a) primary recovery (b) and overall recovery for three ores in the process water at pH 11.2. 51
Figure 4.12: Effect of salinity on (a) primary and (b) overall bitumen/solids ratio of the froth extracted from three ores in the process water at pH 11.2. 52
Figure 4.13: Effect of salinity on the degree of bitumen liberation (DBL) from the (a) Sun08, (b) MA and (c) AE13 ores in the water at pH 11.2. 53
Figure 4.14: Images of bitumen liberation for Sun08, (a) at pH 8.5 without NaCl adding; (b) at pH 8.5 with 4000 ppm NaCl adding; (c) at pH 11.2 without NaCl adding; and (d) at pH 11.2 with 4000 ppm NaCl adding. 54
Figure 4.15: Effect of salinity on dynamic and static contact angles of bitumen recession from a glass microsphere in simulated process water of pH 11.2. 55
Figure 4.16: Effect of salinity on bitumen aeration at pH 8.5 and pH 11.2 with fines addition. 56
Figure 4.17: Effect of salinity on zeta potentials of oil sands fines and VDU bitumen in the tailings water. 57
Figure 4.18: (a) Primary and (b) overall recovery from blends of high grade Sun08 and low-grade AE13 ores in the presence of 4000ppm NaCl at pH 8.5 60

Chapter 1: Introduction

1.1 Oil Sands

Oil sands, also called bituminous sands or tar sands, are a mixture of bitumen (i.e. an extremely viscous form of petroleum), mineral solids (sands and clays) and water. Typically, oil sand ore contains around 6-16 wt% of bitumen, 80-87 wt% of solids and 2-7 wt% of water, [1] depending the origin of the ore. As proposed by Takamura, [2] these components of oil sands are intermixed and there exists a thin layer (about 10 nm) of water film between bitumen and sand particle. The hypothesized structure of oil sands is shown in Figure 1.1.

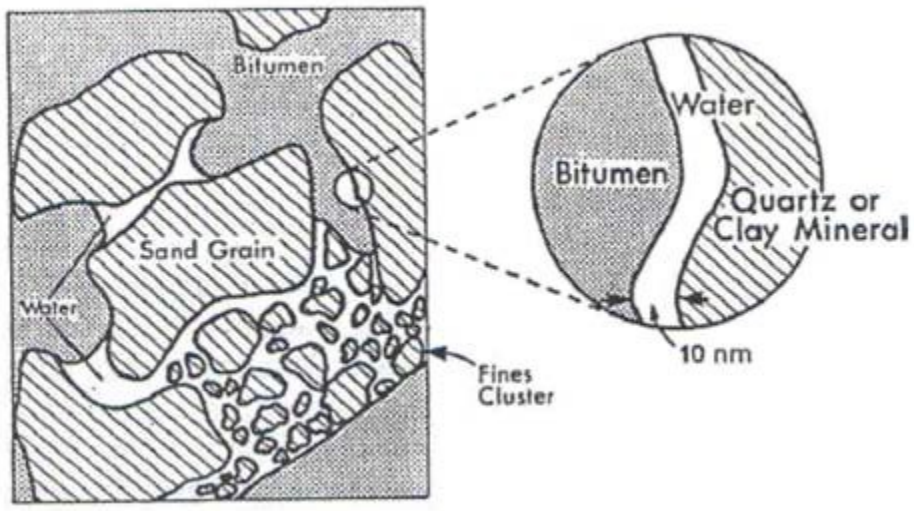

Figure 1.1: The microscopic structure of Athabasca oil sands proposed by Takamura.[2]

The largest oil sands deposits are located in northern Alberta of Canada, with a proven reverse of around 170 billion barrels of crude bitumen, ranking the third largest in the world behind Saudi Arabia and Venezuela.[3] The current level of Alberta's oil sands

production, accounting for 56% of total Canadian oil output, is about 1.98 million barrels per day (mbd); the oil sands production is forecasted to grow to 5.2 mbd by 2030.[4] The abundant oil sands resources will make Canada to be one of the biggest petroleum powerhouses in the foreseeable decades, providing a sustainable energy supple and the great opportunities for Canadians and the entire world.

1.2 Bitumen Production

There are two commercial techniques of extracting bitumen from oil sands — surface mining and in situ thermal technologies, largely depending on the depth of the deposits. For the deposits that are less than 75 m to the ground, *surface mining* method is used to produce crude bitumen, using the Clark Hot Water Extraction (CHWE) process. To recover bitumen from the reservoirs over 75 m depth underground, the *in situ* technique that effectively decreases the bitumen viscosity and increases its mobility usually by injecting stream is employed. The two common in situ methods are steam-assisted gravity drainage (SAGD) and cyclic steam stimulation (CSS).[6] In SAGD invented by Roger Butler and colleagues at Imperial Oil in the 1970s, a set of parallel (one topping the other) and "L-shape" wells are drilled into the oil sands formation. The steam is injected into the upper well, leading to the dramatically lower bitumen viscosity, so that the liquidized bitumen flows into the lower well where it is pumped to the processing plant above the surface through the producer wellbore for further treatment.[5] The CSS is similar to the SAGD. However, the CSS consists of three stages, the second stage of soaking the deposit by

steam.[7] The benefit of the CSS is its higher productivity in deeper reservoirs, but it is not a continuous production process and is highly restricted by the geography of oil sands deposits.[7] Although the in situ operation is a promising technology that targets bitumen from deeper formation, surface mining is currently the major method that many industrial companies use for bitumen extraction. In the next section, the general flowchart of this water-based bitumen extraction (WBE) process is outlined, taking the commercial CHWE as an example since the main procedures of aqueous extraction are rather similar. (Details of the fundamental sub-steps of the WBE are described in Chapter 2.)

1.2.1 Hot/Warm Water-Based Bitumen Extraction

Figure 1.2 shows a typical flowchart of bitumen extraction process based on hot water (also known as *Clark Hot Water Extraction*, CHWE), which was initially developed by Dr. Karl Clark and implemented commercially by Suncor Energy Inc. and Syncrude Canada Ltd.. The process is as follows: Shovels and trucks are used to mine the open-pit oil sands. The mined oil sands are then crushed into smaller pieces and mixed with hot water of typical temperatures of 75ºC to 80ºC and process aids (normally caustics), in a mechanical agitation tumbler to allow the slurry conditioning.[3] With the advent of hydro-transport pipeline system that replaces the tumbler, the process operating temperature has been reduced to about 50 ºC: this is referred to as *warm water bitumen extraction* (WWBE) process. During the slurry conditioning, bitumen is ready to liberate from sand grains and the liberated bitumen droplets are

allowed to attach to air bubbles under a favorable process condition.

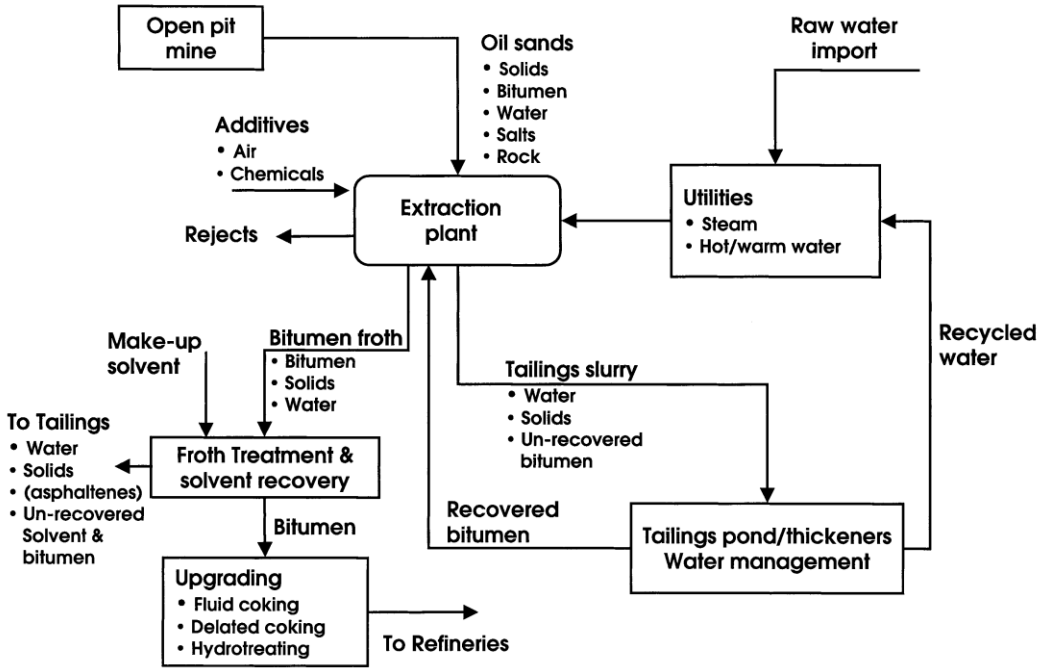

Figure 1.2: Generalized scheme for oil sands processing using hot water based extraction process. [3]

The conditioned slurries are sent to the primary separation vessels (PSV) where the aerated bitumen with inherent air would float to the top of the PSV, despite no air addition at this stage. The middle part in the PSV is called middling that usually contains a small amount of bitumen and is considered profitable for further recovery of bitumen. Normally, a second flotation is employed for the middling from the primary flotation cell (PFC). With inducing air into the cell, the small amount of bitumen attached to the air bubble is able to float to the top where it is recovered as froth. The collected froth, usually at lower bitumen froth quality, is gone back to the PSV, while the remaining materials are fed into tailings stream along with the bottom

part in the PSV for screening and prior to flotation in the secondary flotation cell (SFC). The obtained bitumen from SFC is also sent to the PSV. The primary froth which usually has around 60wt% bitumen, 30wt% water and 10wt% solids, are flown to the de-aerator, then screened and placed into the tanks for the froth treatment. Solvent, such as paraffin or naphtha, is added to dilute the froth. Next, the diluted froth is centrifuged to get rid of the remaining large amount of water and solids. Finally, the treated froth is delivered to upgrading units. The remaining materials in the SFC are discharged to the tailings pond for settling. As mentioned earlier, different company may have different procedures for the bitumen extraction and froth treatment, but the main concept is the same. One of the main disadvantages of the hot/warm water extraction method is that it consumes a huge amount of water, and produces plenty of tailings which need to be treated. The tailings pond is now extensively expanding, and the treatment of tailings costs a great deal of capital and operational cost or causes many environmental concerns.

1.3 Tailings and Water Treatment

Tailings are the left-over materials after the process of separating the valuable fraction from the uneconomic fraction of an ore. [8] The oil sands tailings slurry is a muddy suspension of solids (sands and clays), unrecovered bitumen, soluble organic materials and salts co-existing in the alkaline environment. [9] More than 200 million liters of mature fine tailings are produced each day, and tailings are stored indefinitely in open lakes that cover an area approximately 50% larger than the city of Vancouver.

[10]

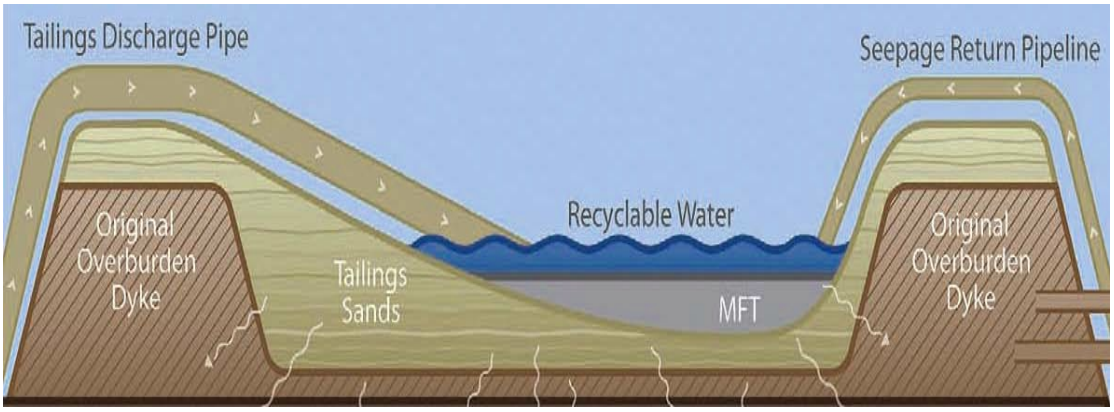

Figure 1.3: Scheme of Tailings Pond

As shown in Figure 1.3, the tailings ponds are to store the discharged tailings slurry from extraction plants. The dense solids segregate to form the dykes, however, the majority of fine particles and water remain as suspensions. [4] A layer of mature fine tailings (MFT) forms after two or three years. The MFT consolidates extremely slowly. [4] The complete settling process for the MTF is anticipated to take over ten decades. [4] Therefore, the acceleration in the settling rate of the tailings has been attempted using numerous methods, in order to gain more recycling water and reduce the volume of tailings ponds. [4] There are several physical mechanical treatment methods for volume reduction of Clark Hot Water Extraction fine tailings, such as centrifugation, filtration, electrophoresis, electro-coagulation, and sonic waves. More commonly, several chemicals such as inorganic coagulants and organic flocculants are employed for the treatment. The approaches are referred to as chemical methods. [4]

Among those various methods, there are two main commercial techniques widely used in the tailings treatment. The first is via calcium sulphate (gypsum) addition to

treat the fine tails, from which the *composite tailings* (CT) technology was been eventually developed. This technology is designed to deposit the slurry to release water rapidly with no segregation.[11] Unfortunately, the recycled water from the CT treatment contains high concentration of calcium ions that are detrimental to the extraction process. The second is called as the *paste* technology. By avoiding adding divalent ions into tailings treatment, organic polymer(s) is applied in the paste technology instead. The main concept of paste technology is through flocculation, i.e. destabilizing the dispersion by bridging of the colloidal particles together with polymeric flocculant(s). The main functions of flocculant(s) involve polymer-bridging, charge neutralization, polymer-particle surface complex formation, and depletion flocculation.[12, 13] The paste treatment can bring a clearer supernatant and more consolidated sediment by enhanced settling of fine tails;[4] this sediment is referred to as thickened tailings (TT).[4, 14]

1.4 Problem Identification: Water Salinity

Obviously, the maximum bitumen recovery efficiency and "clean" water recycling from the tailings pond are the two main integrated tasks that the oil sands industries want to accomplish. Many physical and chemical processing factors must be considered to promote (or at least not depress) high bitumen recovery. Among these factors, chemistry (i.e., type and concentration of ions) of process water is one of key parameters that affect the processability of oil sands ore.[4] As described earlier, in the WBE process, caustic — usually sodium hydroxide is used as the proces aid to

increase the bitumen recovery. The intension of adding caustic is to alter the pH of the process water in which bitumen liberation from sand grain is intensified due to the synergistically increased surface charges on both the bitumen and sand grains. The enhanced electric repulsive force generates a much stable bitumen phase and clays suspensions, therefore preventing slime coating, which in turn enhances the bitumen and air bubble attachment efficiency. Meanwhile, adding sodium hydroxide can precipitate the divalent cations in the process water, such as calcium ions (Ca^{2+}) and magnesium ions (Mg^{2+}) which are known to be harmful to the extraction process. Higher pH also helps release more natural surfactants from the bitumen, reducing the interfacial tension between water and bitumen, thermodynamically favors the bitumen liberation.

On the other hand, the sodium originating from the added caustic is eventually discharged into the tailing pond where the water is recycled. By considering the repeated recycling of the process-affected water from the pond as demonstrated in the right-side line of Fig. 1.3, the sodium ions in the process water will inevitably increase, due to the addition of sodium hydroxide as well as the ion exchange or releasing from the oil sands ores. Unlike divalent cations, sodium ions cannot be precipitated out from the process water. The only consequence is the gradually increased sodium concentration. It was revealed that the salinity of tailings pond water (TPW) was increased at a rate of 75 mg/L per year from 1980 to 2001.[15] The oil sands industry is concerned that the increasing water salinity will potentially affect

the bitumen recovery from the mined oil sands ores. This is also the motivation of this study. From an economic view, a 1% reduction in bitumen recovery is estimated to be equivalent to a loss of 1.44 million US dollars daily, at current operational outputs. [16] In terms of the environment, the unrecoverable bitumen ended up in the tailings creates a big environmental threat. Thus, understanding the effect of salinity on bitumen extraction and finding a solution to resolve its negative effect are of great importance from both the economic and environmental prospective.

1.5 Thesis Objectives

The main objective of the current study is to investigate the impact of salinity on bitumen recovery from different types of oil sands ores using a bench-scale flotation cell in the warm water-based bitumen extraction (WWBE) process. Additionally, the fundamental sub-processes of extraction — bitumen liberation and aeration are studied to obtain a better understanding of the salinity effect on the whole extraction process. The pH effect is also evaluated to determine whether altering pH is a solution for the salinity issue. Finally, blending of good and poor processing oil sands ores is investigated to minimize the negative impact of increasing salinity.

1.6 Thesis Outline

This thesis is organized as follows:

Chapter 1: The general oil sands production and water-based bitumen extraction are

briefly introduced. This is followed by the motivation of this thesis (i.e., identifying the importance of water salinity on the WBE), objectives and structure of the thesis.

Chapter 2: A summary of related literature research is presented. The main aspects include the principles of colloid science associated with oil sands research, and its effect on bitumen recovery, bitumen liberation, aeration, etc.

Chapter 3: Materials used for this study are presented, followed by the procedures of experiments including bitumen flotation by Denver Cell, dean stark for product, in situ bitumen liberation visualization, contact angle measurement, induction time, and zeta-potential measurements.

Chapter 4: The effect of salinity on bitumen recovery of three different types of ores as well as the remediation to the salinity issue is demonstrated. The results of bitumen liberation, aeration, zeta-potential measurements are given to explain the of sodium ion addition on bitumen recovery effect.

Chapter 5: The effect of salinity on the warm water-based extraction is concluded based on the results obtained using three different types of ore. The suggestion for the future work is also included.

Chapter 2: Literature Review

2.1 Colloids

Colloid is defined as a dispersion of particles smaller than a set unit (the dividing line is not strict in literature and could be 10 μm or 100 μm), [17] including suspension, emulsion, sol and gel. Several types of colloids — oil-in-water and water-in-oil emulsions and aqueous fine clay suspensions are often formed in the oil sands processing systems. For example, in oil sands extraction, oil sands are mixed with hot water. As mixing continues, larger oil sands lumps are turned into small dispersed particles. In the froth treatment, the emulsified water in diluted bitumen is targeted to be removed to minimize the corrosion problem to the upgrading facilities. The interfacial area increases with decreasing particle sizes; it eventually begins to control the properties of the system. The interactions between these small particles determine the bitumen recovery and froth quality. In the natural case, the air bubbles and the bitumen droplets are hydrophobic or lyophilic, while the sand grains embedded in Alberta's oil sands are hydrophilic or lyophobic. Hydrophilic and hydrophobic are the two well-known terminologies in colloidal science, classified by Freundlich [18, 19], as water loving and water hating, respectively. In such case, bitumen can be floated by the air bubbles due to the significantly lower apparent density, while the sand grains stay in the bottom of the PSV. The interactions between particles in a oil sands system is rather complex. Understanding the fundamental theories of colloidal science is of great importance for us to manipulate influencing factors and apply them on the oil

sands extraction.

2.2 Electrical Double Layer and DLVO Theory

In aqueous extraction environment, solids (mostly quartz) immersed in the water are negatively charged due to the dissociation of a proton from a surface hydroxyl group.[20] The following chemical association/dissociation equation occurred at the sand-water interface is taken as an example:

$$SiO_2 + H_2O \rightleftharpoons (H_3SiO_3)_s \rightleftharpoons (H_2SiO_3)^-_s + H^+ \quad (2\text{-}1)$$

This chain of events negatively charges the solid surface, as the dissociating H^+ ion carries away a positive charge and leaves the negative charge behind. The equilibrium is shifted to the right, resulting in a higher negative charge of the silica surface at high pH condition.[17] The similar dissociation mechanisms are involved in the charging of all oxide-type minerals, e.g. clays, alumina, and many others.[17] Due to the electrical neutrality for the whole system, the aqueous phase near the solid surface is positively charged.[17] The negatively charged solid surface attracts cation-ions in the solution, forming a layer as *electrical double layer* (EDL).[17] A Stern model is widely used to describe the profile of electrical potential distribution near the charged surface as shown in Figure 2.1.[19-22] This model suggests that the EDL consists of two separate regions — the inner Stern layer and the outer diffuse layer. The Stern layer is the region close to the surface, where counter ions are bounded near the surface due to special-adsorbing and Coulomb interactions. The diffuse layer is the region next to the Stern layer and ions in the diffuse layer are highly movable. [20] As illustrated in

Figure 2.2, the Stern potential decreases linearly with the distance from the solids surface while the potential beyond the Stern plane decreases exponentially. The mobile boundary of the diffuse layer is the plane of shear and the potential at the shear plane is called the *zeta potential* (denoted as ζ) — an important parameter of controlling colloidal stability.

Roughly 70 years ago, the four pioneer scientists Derjaguin, Landau, Verwey and Overbeek developed a theory to explain the aggregation of aqueous dispersions quantitatively. [19] This is the well-known *DLVO theory* in which the coagulation of dispersed particles is explained by the interplay between two forces: the *van der Waals forces* and the *electrostatic double-layer forces* — sometimes referred to as DLVO forces. Typically, van der Waals forces are attractive and promote the coagulation while the double layer-forces are repulsive and stabilize the dispersions.[19]

Figure 2.3 shows the interaction energy between two identical spherical particles calculated using the DLVO theory. In general, it can be described by a very weak attraction at large distances (secondary energy minimum), an electrostatic repulsion at intermediate distances, and a strong attraction at short distances (primary energy minimum).[19] Adding salt reduces the electrostatic energy barrier, and van der Waals attraction dominates, leading to coagulation, aggregation, and precipitation. If applying onto oil sands extraction, the lower bitumen recovery and froth quality

would be expected when the system has higher salt concentration due to the depressed electrical repulsive force between bitumen and clays.

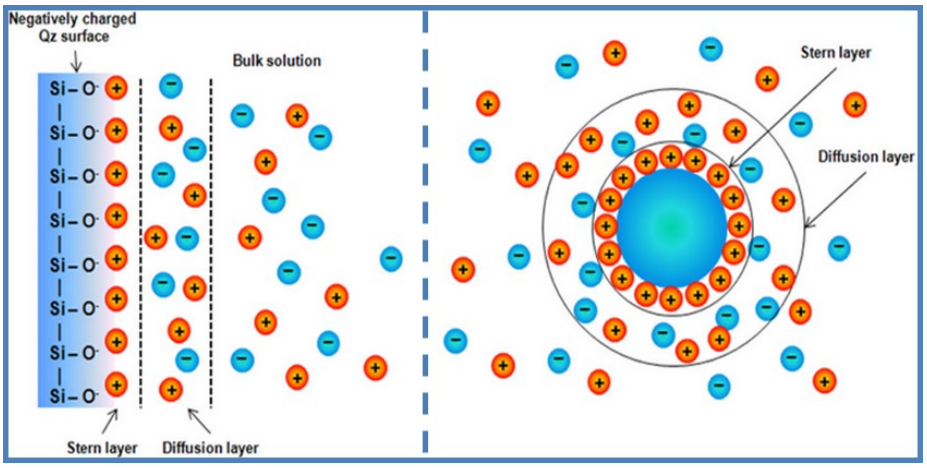

Figure 2.1: Schematics of electrical double layer based on Stern model.

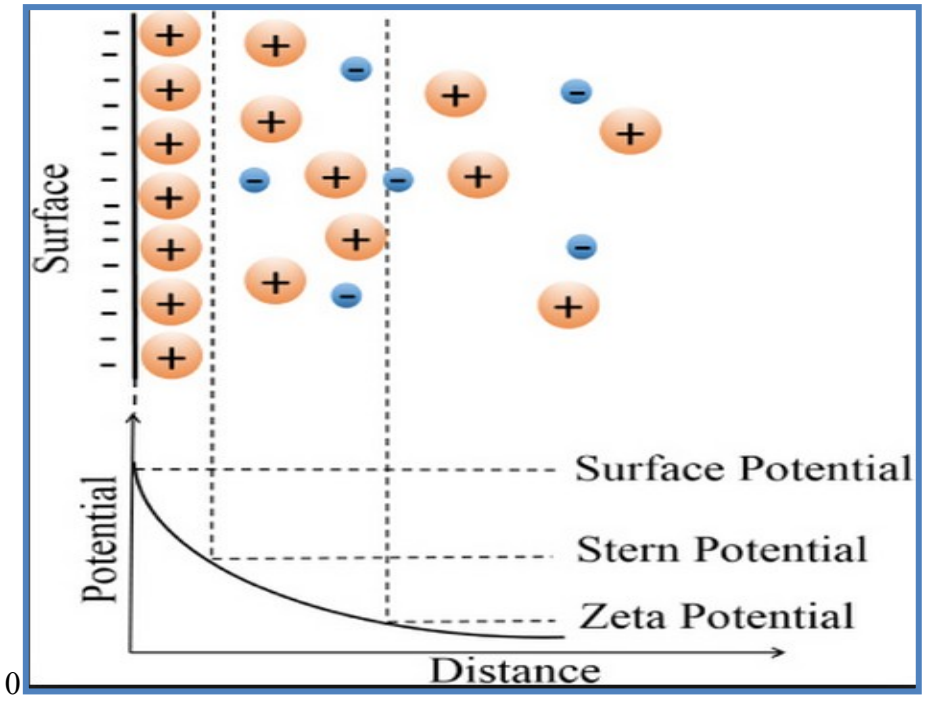

Figure 2.2: The profile of the three potentials in the Stern model. [19]

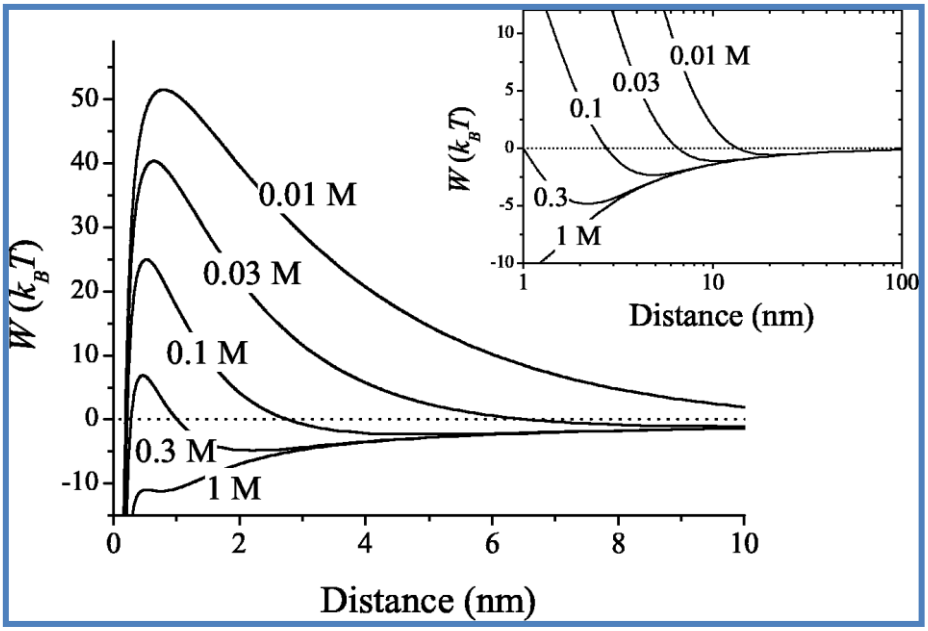

Figure 2.3: Gibbs free energy (normalized by k_BT) of interaction versus distance for two identical spherical particles of R = 100 nm radius in water, containing different concentrations of monovalent salt. The calculation is based on DLVO theory. The Hamaker constant $A_H = 7\times10^{-21}$ J, surface potential ψ_0 = 30 mV. The insert shows the weak attractive interaction (secondary energy minimum) at very large distances.[19]

2.3 Fundamentals of Bitumen Extraction

In order to achieve the effective bitumen recovery using the WBE process, the prerequisite is that bitumen should be separated from the sand grains, which called *bitumen liberation*. Simultaneously, bitumen droplets collide with dispersed air bubbles, resulting in the formation of bitumen-air aggregates which readily float to the top of the PSV. This step is called *bitumen aeration*. These fundamental steps are essential to bitumen recovery. Any process parameters that hinder any of these steps will have a negative impact on the overall bitumen recovery process. [17]

2.3.1 Bitumen Liberation

As shown in Figure 2.4, bitumen liberation can be broken down into two subprocesses: bitumen recession on the sand surface in water, and bitumen separation from the sand grain. [23]

Figure 2.4: Schematic of bitumen liberation from a sand grain.[23]

During the liberation process, the initial bitumen-sand grain interface is replaced as water advancing on the surface of sand, with small bitumen droplets forming on the sand surface; this is termed as bitumen recession. With the assistance of external mechanical (hydrodynamic) forces, the recessed bitumen would be easily detached, although bitumen detachment is thermodynamically unfavorable. If the criterion that the sand-water interaction is stronger than bitumen-sand interaction is satisfied, bitumen recession is favorable. In other word, bitumen recession requires the water-loving (hydrophilic) solid surface. The extent of bitumen recession is often characterized by the contact angle measured from the aqueous phase at three-phase contact (TPC) line at equilibrium stage, illustrated in Figure 2.5 as an ideal example. Obviously, the lower the equilibrium contact angle, the more beneficial to bitumen

recession.

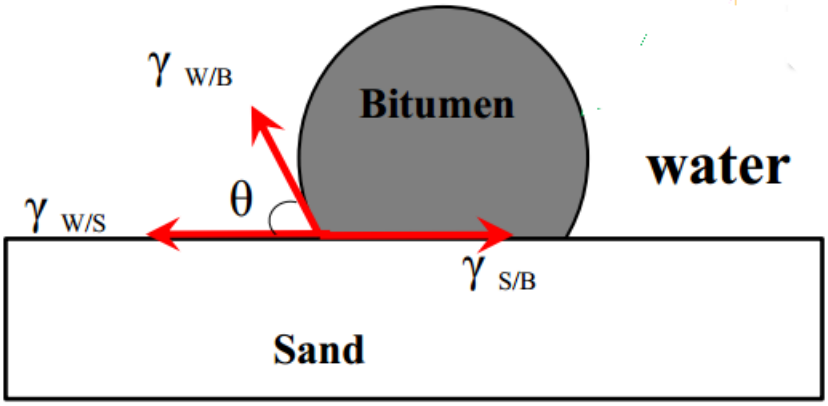

Figure 2.5: Aqueous contact angle of bitumen on a sand grain.[26]

According to the Young's equation, the equilibrium contact angle θ is associated with the surface energies (i.e. interfacial tensions γ) at three interfaces:

$$cos\theta = (\gamma_{S/B} - \gamma_{W/S})/\gamma_{W/B} \quad (2\text{-}2)$$

where subscripts B, S, W represent bitumen, solid, and water phases, respectively. It is revealed from the above relation that the way of obtaining the lower equilibrium contact angle (therefore the enhanced ultimate degree of bitumen liberation) is to decrease bitumen-water interfacial tension or/and the sand-water interfacial tension (since bitumen-solid interfacial tension is almost constant at normal operating condition). On the other hand, the dynamics (i.e. rate) of bitumen recession depends not only on the interfacial tension, but also on the viscosity of bitumen.[24; 51]

Previous studies have indicated that bitumen liberation is influenced by various process variables — e.g., conditioning temperature, agitation speed, water pH and

chemistry of process water. The pH effect was examined by Basu et al.. [26] In their study, a layer of bitumen was coated on the glass surface that mimicked the sand grain, and then immersed in the aqueous solution. The contact angle was measured as a function of pH. The equilibrium contact angle was decreased as aqueous pH increased. This was attributed to the underlying mechanism that higher pH facilitates the hydrolysis and charging of sand water interface, and the release of surface active surfactants from bitumen, [26] resulting in the reduction of the water-solid and bitumen-water interfacial tensions. Basu et al. also studied the effect of NaCl on bitumen displacement by water on a flat glass surface. [26] Their result suggested that above certain sodium concentration, bitumen displacement was hindered. The depressing of bitumen displacement was found to be more pronounced at higher pH when salt was added, suggesting the effect of NaCl was more prominent at higher pH. Sundeep et al. investigated the bitumen liberation from real oil sands by online visualization. It was demonstrated that the degree of bitumen liberation was decreased by high sodium concentration. [27] Liu et al. measured the inter-molecular forces between bitumen and silica tip in aqueous solutions of different amount of KCl. The increasing salt concentration was claimed to reduce the repulsive forces between bitumen and silica, demonstrating that salt addition resulted in a compression of electrical double layers. [28]

2.3.2 Bitumen Aeration

Bitumen aeration is the process of bitumen attachment to air bubbles. After liberation,

bitumen droplets would remain suspended in the slurry if they were not aerated. Through aeration, the apparent density of bitumen-air mixture is reduced and much lower than that of the separation medium, triggering the aerated bitumen to float to the top of the slurry in the separation vessel where bitumen-rich froth can be recovered. [29] This process is illustrated in Figure 2.6. There are two possible scenarios of bitumen aeration — bitumen-air attachment and air engulfment by bitumen, depending the operation condition.

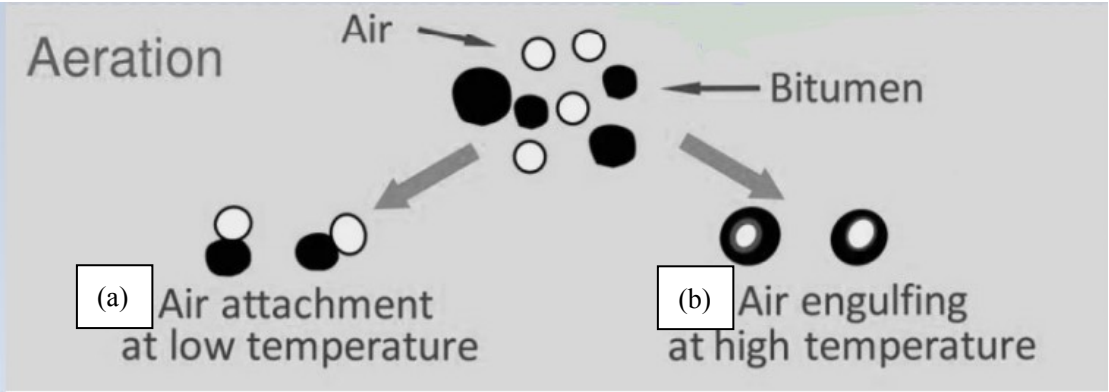

Figure 2.6: Schematics of (a) bitumen-air attachment and (b) air engulfment.[29]

From the thermodynamic point of view, the process of bitumen attaching to air bubble is favorable. The Gibbs free energy change ΔG with an attachment area A is given by:

$$\frac{\Delta G}{\Delta A} = \gamma_{B/A} - \left(\gamma_{B/W} - \gamma_{A/W}\right) \tag{2-3}$$

where subscript A is air bubble. Based on the Young's equation, the formula (2-3) can be further transformed into:

$$\frac{\Delta G}{\Delta A} = \gamma_{A/W}(cos\theta - 1) \tag{2-4}$$

The change of the free energy with area is always negative. However, in terms of a

kinetic point of view, bitumen aeration is believed to consist of three steps: air-bitumen collision, water thin film thinning, and water film rupture and formation of a stable attachment. [30,31] When an air bubble is approaching to a bitumen surface, the thin water film barrier between bitumen surface and air bubble would potentially prevent their attachment. The barrier can be originated from the surface forces and hydrodynamic forces between the two surfaces.[32,33] Since the bitumen surface and air bubble are both negatively charged at an alkaline condition, the electrical double layer forces between them are repulsive, so are the van der Waal forces of bitumen and bubble in the electrolyte due to the negative Hamaker constant. Based on the classical DLVO theory, a collective high repulsive barrier is anticipated, which is not suitable for explaining the bitumen and air bubble attachment. The extended DLVO theory considering other forces such as attractive hydrophobic force and attractive binding force is often adapted. [34-37]

The attractive forces that are generated from the surface hydrophobicity contribute to the main driving surface force for the bitumen-bubble attachment. Hence, the efficiency of bitumen aeration is well related to the contact angle of bitumen substrate in a system. Adamson and Gast measured the contact angle (see Figure 2.7) of water on bitumen as a function of aqueous pH.[36] The authors found that increasing pH decreases the contact angle of water on bitumen, indicating that higher pH provides a less favorable condition for air bubble attachment to bitumen.

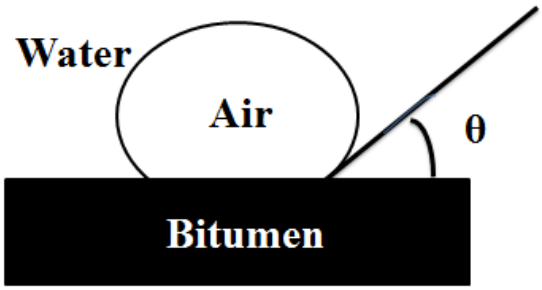

Figure 2.7: Aqueous contact angle of air bubble on bitumen surface.

Similarly, Zhou et al. studied the relationship between the contact angle of bitumen and air bubble in aqueous phase and the bitumen recovery. [39] The result showed that recovery was related to the contact angle and higher recovery corresponded to the higher contact angle measured from aqueous phase. The bitumen surface hydrophobicity played an important role. Gu et al. measured the induction time of bitumen and air bubble, defined as the minimal contact time required for bitumen-air attachment, as a function of divalent ions (calcium) concentration. [37] The results in Figure 2.8 show that higher concentration of calcium ions promoted bitumen aeration when the system contained no fines. However, the situation was converted when the fines were presented in the system. This was explained by the fact that calcium ions would be able to bridge the bitumen surface and fines, with fines preventing the bubbles from attaching to the bitumen surface as shown in Figure 2.9 for the illustration. Additionally, it was revealed that the size of air bubble was critical to aeration. The smaller the size of the air bubbles are, the more efficient the aeration will be.

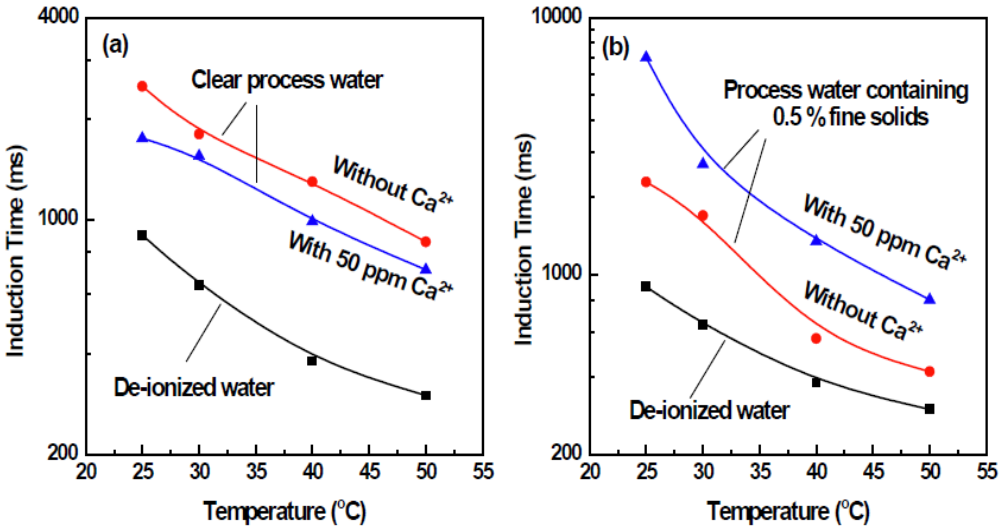

Figure 2.8: Induction time of air-bitumen attachment as a function of temperature: (a) in clear process water and (b) in process water containing 0.5 wt% fines.[37]

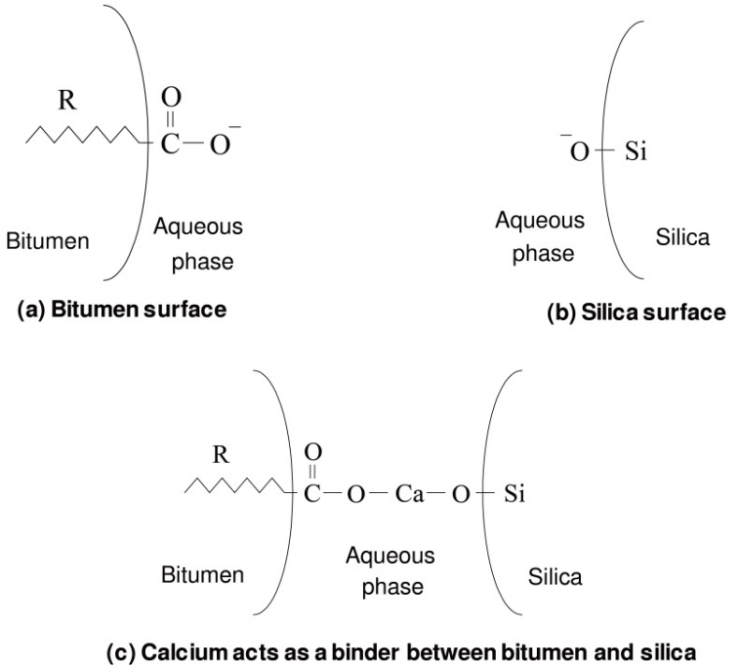

Figure 2.9: Schematics showing the impact of calcium on silica-bitumen interactions. Negatively charged for (a) bitumen and (b) silica surfaces in alkaline solution; (c) calcium acts as a binder between the silica and bitumen surfaces.[37]

2.3.3 Other Relevant Studies

Hot or warm water based oil sands extraction is a complex system. Many factors would influence the bitumen recovery. The effect of fines content on bitumen recovery varies depending on the type of fines and the water chemistry.[5] Kasongo et al. found that adding both 40 ppm calcium ions and 1 wt% of montmorillorite clays depressed the bitumen recovery for the good ore, while no negative impact was found when kaolinite or illite was added.[38] This was attributed to the swelling nature of montmorillorite.[41-44] Wallace et al. reported that the presence of degraded illite would depress the bitumen recovery.[44] Ding et al. obtained a decrease of bitumen recovery when illite was added in the low pH DI water, but the detrimental impact of illite was relieved by increasing the pH of the aqueous phase.[45] Dang-Vu et al. studied the impact of wettability of the solids in oil sands on bitumen recovery.[46] Results indicated that higher wettability of fine solids would lead to higher bitumen recovery and froth quality. Temperature is another factor that plays an important role in influencing bitumen recovery. Long et al. demonstrated that the bitumen recovery was increased from 10% to 90% when the processing temperature increased from 25°C to 50°C, regardless the nature of the ores,[47] which corresponds well with the increase with the long-range repulsive forces and decrease in adhesion forces between bitumen and fines, and a decrease in induction time of bitumen air bubble attachment. Ren et al. stated that increasing process temperature can restore the reduced wettability of solids due to ore weathering, resulting in the improved bitumen recovery. [48, 49]

Chapter 3: Materials and Methods

3.1 Oil Sands Characterization

Three types of oil sands ores (denoted as Sun08, MA and AE13) were used in this study. The characteristics of these ores in terms of bitumen, water, solids and fine s contents are shown in Table 3.1. Here, fines are defined as mineral solids with less than 44 μm in size and expressed as a percentage of total solids in the ore. All the samples were kept in refrigerator to avoid oxidation. Before each test, the ore was thawed at room temperature for 2 hours.

Table 3.1: Composition (wt%) of oil sands ores.

Ore	Solids	Bitumen	Water	Fines
Sun08	82.8	16	1.2	6
MA	83.5	8.2	8.3	20
AE13	86.8	8.3	4.9	38

Based on the percentage of fines, the three ores can be classified as low-fine (or high grade), medium-fine (medium grade) and high-fine (low-grade) ores. For the further confirmation, the size distribution of solids in these three ores was analyzed by Master-sizer and their general information is shown in Figure 3.1. The size of solids in ore Sun08 was in the largest range, followed by ore MA and ore AE13. The size distribution was in a good agreement with the fines content mentioned in Table 3.1,

with d_{50} from 18.7μm to 187μm for AE13 to Sun08, respectively.

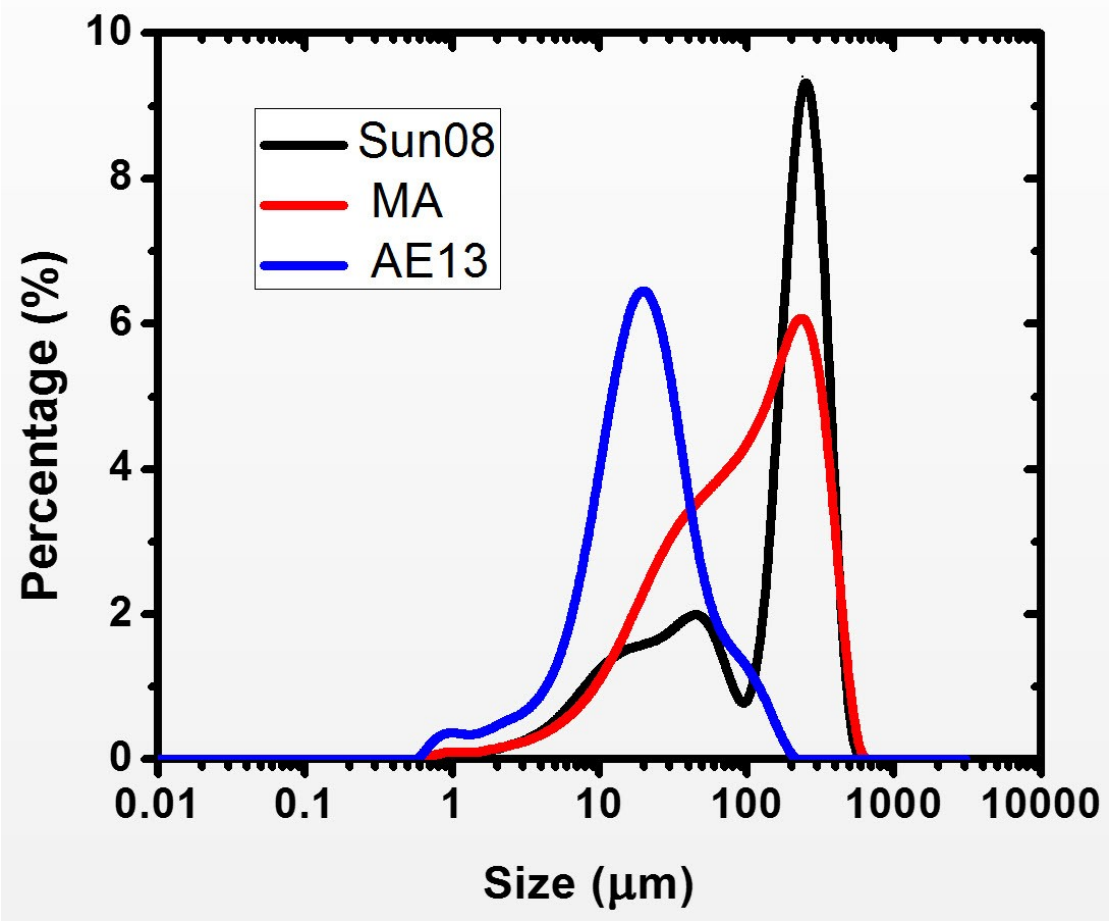

Figure 3.1: Solid size distribution of three ores.

3.2 Chemistry of Process Water

In order to make experimental condition close to the operating conditions of the oil sands industry, the industrial recycle process water provided from Aurora plant of Syncrude Canada was used in flotation tests. The pH of the process water was controlled at 8.5 and 11.2 by the base sodium hydroxide and the acid hydrogen chloride (both of analytical grade and purchased from Fisher Scientific). The concentration of major cation ions and natural carboxylic surfactant (CS) of the process water is given in Table 3.2.

Table 3.2: Average composition of process water

Average Composition of Process Water					
pH	Ca^{2+} (ppm)	Mg^{2+} (ppm)	Na^{+} (ppm)	K^{+} (ppm)	CS (10^{-5}mol/L)
8.5	40	17	660	23	25

3.3 Mineralogy of Clay Fines

Clay fines supplied by Teck Ltd., which are known to be detrimental to the oil sands extraction, were used in the experiments for the induction time measurements. The respective clay mineralogy that was also provided by Teck Ltd. is given in Table 3.3.

Table 3.3: Clay mineralogy for the fines used in the induction time measurement.

Composition	Coarse fraction (wt%)	Fine fraction (wt%)	Overall (wt%)
All solids	59.86±6.63	40.14±6.63	100±0.00
Total Clay	19.40±5.47	88.97±5.41	47.33±1.08
Quartz	77.00±5.67	11.03±5.41	50.51±1.26
K-feldspar	1.14±0.81	-	0.67±0.43
Plagioclase	0.41±0.08	-	0.25±0.08
Calcite	0.54±0.20	-	0.33±0.16
Dolomite	0.31±0.12	-	0.19±0.10
Siderite	0.73±0.13	-	0.44±0.09
Pyrite	0.46±0.29	-	0.29±0.22
Chlorite	0.75±0.05	2.45±0.28	1.42±0.04
Kaolinite	6.02±1.81	46.30±2.81	22.22±1.51
Illite	12.63±3.76	38.64±4.65	23.05±2.07
Illite/Smectite Mixed Layer	0.00±0.00	1.58±0.27	0.64±0.19

3.4 Experimental Methods

3.4.1 Bitumen Flotation

The bitumen extraction tests were performed using a Denver flotation cell as shown in Figure 3.2 This cell consisted of a 1-L stainless steel cell, an impeller, and a 1/2 HP Baldor industrial motor. As illustrated in the schematics of Figure 3.2, the protocol of bitumen extraction in this study is described as follow: For each test, 500-g of the thawed ore was added into the flotation cell with 250 mL of process water with desired pH value at 80°C, leading to the resultant slurry at 50±1°C. In the process water, different amount of sodium chloride (Reagent-grade, Fisher Scientific) ranging from 0 to 4000 ppm was added. After agitating the oil sands slurry at the rate of 1500 rpm for 5-minute, the water bath was attached to the Denver cell to maintain the constant operating temperature at 50°C. The air flow rate was kept at 80 mL/min. After completing the conditioning stage, 800 mL of the same process water at 50°C was added into the cell. After agitating at the same speed for 10 minutes without air input, the primary bitumen froth was collected. Secondary froth was collected after another 5 minutes agitation at same speed but with 150 mL/min air supply. After the froth collection, the left-over slurry remained in the Denver cell was discharged as tailings. The primary and secondary froth collected and placed in the thimbles was further analyzed using the Dean Stark apparatus as described next to determine the mass amount of bitumen, water and solids in the froth.

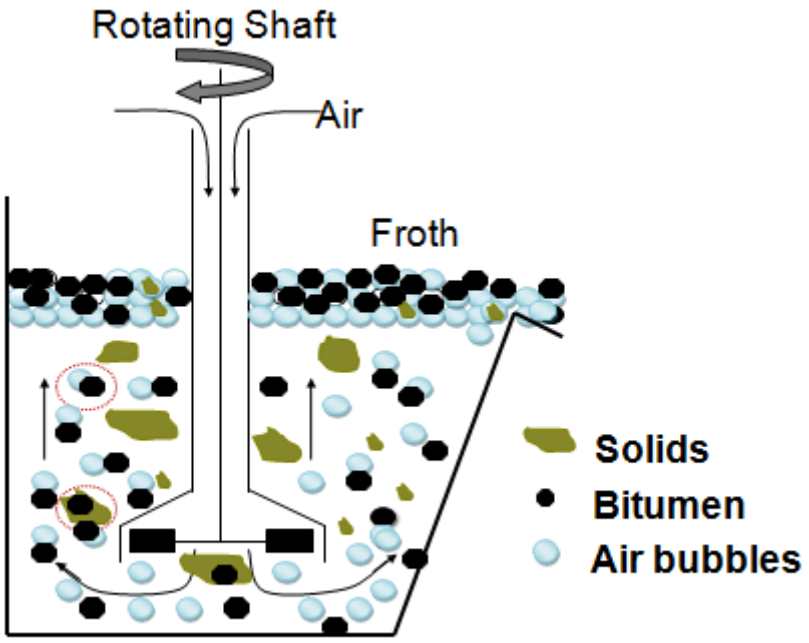

Figure 3.2: Scheme for the Denver flotation cell.

3.4.2 Dean Stark Analysis

Dean Stark analysis is the most common method to determine the mass amount of bitumen, solid and water that can be used to evaluate bitumen recovery and froth quality from the primary and secondary froth of the bench-scale flotation. Whatman thimble (Fisher Scientific) with the bitumen froth is placed in a steel wire holder, with a mesh lid on the top of the thimble. This assembly is then placed in a large extraction flask, on top of which a condenser is connected aside with a trap. About 200 mL toluene was poured into the extraction flask. With the heater on, toluene is heated and vaporized to the condenser, so is water in the froth. The condensed water, due to its higher density, accumulates into the trap, while the condensed toluene over-flows back to the thimble and extracts bitumen from the froth into the extraction flask, with the solids solely remaining in the thimble in the end. The completeness of Dean Stark

extraction was indicated by the two points: (1) The dripping toluene from the thimble bottom was clear; and (2) There was no water flown into the trap. After satisfying the two indications and then cooling down, the thimbles were transferred into the vacuum oven for overnight to dry the solids. A small glass bottle was used to collect the water in the trap, and the mass of the water was weighed. The residue dark toluene-bitumen solution was then transferred into a 250-mL volumetric flask, with toluene being filled up to 250 mL. After homogenizing, 5 mL of diluted bitumen solution was taken using a pipette and placed evenly on a filter paper. Waiting for 20 minutes in the fume hood, the difference of the filter paper with and without (w/o) bitumen was measured to determine the mass of bitumen in the froth. From there, the bitumen recovery rate and froth quality in term of bitumen: solids (B/S) and bitumen: water (B/W) ratios could be easily obtained as follows:

$$Recovery\ (\%) = \frac{mass\ of\ bitumen\ in\ the\ froth}{mass\ of\ bitumen\ in\ the\ ore}$$

$$= \frac{weight\ difference\ of\ the\ filter\ paper\ w/o\ bitumen \times 50}{weight\ of\ ore \times precentage\ of\ bitumen\ in\ the\ ore} \times 100\%$$

$$B/S\ Ratio = \frac{mass\ of\ bitumen\ in\ the\ froth}{mass\ of\ solids\ remaining\ in\ the\ thimbles}$$

$$B/W\ Ratio = \frac{mass\ of\ bitumen\ in\ the\ froth}{mass\ of\ water\ collected\ in\ the\ glass\ bottles}$$

3.4.3 Bitumen Liberation

Bitumen liberation experiment was conducted using an in-situ bitumen liberation flow

visualization cell (BLFVC) developed by Sundeep et al. [27] in our research group. The experimental setup is shown in Figure 3.3. For each test, a small amount of (approximately 1 g) thawed oil sands ore was placed in the sample holder and the surface was flattened with a small hammer. The process water as the feed solution with desired water chemistry was stored in a small beaker. A peristaltic pump (Masterflex, C/L) was used to circulate the process water through the liberation flow cell. The liberation process was monitored and recorded using a stereo-optical microscope from Olympus (SZX 10) connected to a high-resolution charged-coupled device (CCD) camera. For all the tests, the flow rate of water was controlled at 5 mL/min and the temperature of water bath was controlled at 23°C, unless otherwise stated.

Image-pro software was used to analyze the frame pictures extracted from the recorded video. For each ore, a defined threshold was determined case by case to distinguish the liberated area on the image. Briefly, as illustrated in the flowchart in Figure 3.4, the extracted image was first converted to gray scale format, and then the threshold was applied to the gray scale image by Image-pro. The pixel in the image was known to contain a specific value according to its color, ranging from 0 (representing the pure black) to 255 (pure white). Here above the threshold was considered to be liberated area. The degree of bitumen liberation (DBL) was then defined as the ratio of white area to the whole image area. Taking an example as shown in Figure 3.5 where the original and grey-scale images of bitumen liberation

were taken at different time for a good ore. At time = 10 s the original image was quite dark, and the respective gray scale format was almost black. However at time = 250 s, the original image possessed a few bitumen on the surface. The gray scale image contained very high percentage of white areas, suggesting a high rate of bitumen liberation.

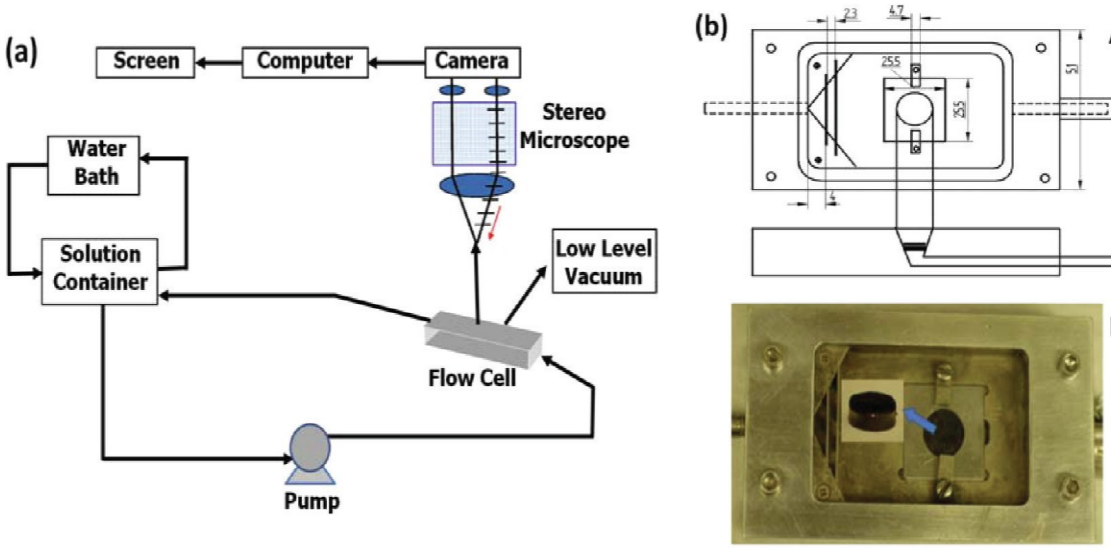

Figure 3.3: Bitumen liberation experimental setup.[27]

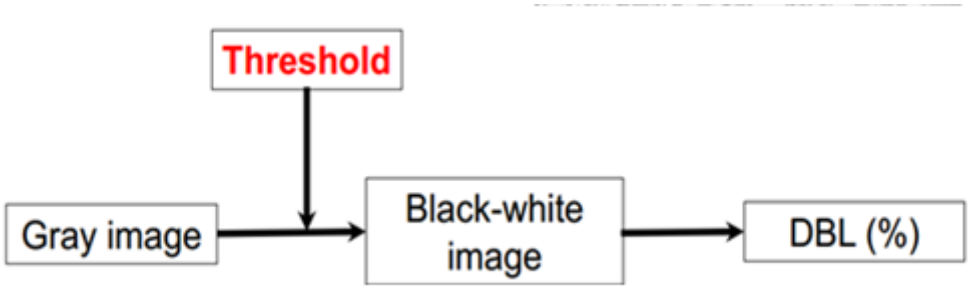

Figure 3.4: Procedure of determining the degree of bitumen liberation (DBL).

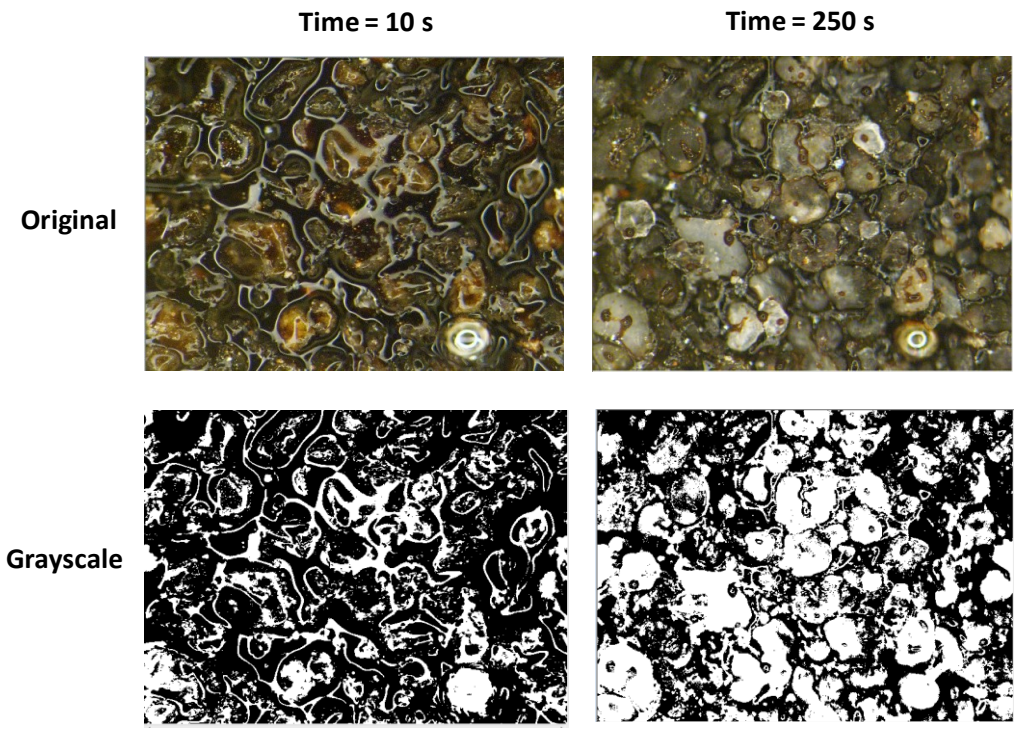

Figure 3.5: Examples showing bitumen liberation image analysis.

3.4.4 Contact Angle Measurement

The contact angle measurement was carried out using a modified micro-pipette technique by analyzing the bitumen droplet relaxation on a spherical glass substrate.[50] Micro-pipette technique was initially introduced by Yeung et al. into the oil sands research.[50] This technique was further modified to suit the requirement of the current study. Here, the procedure of so-called droplet relaxation experiment is briefly described. [51] In this study, the micron-scale and ball-shaped glass tips were coated with bitumen in air. Then the sample was placed into aqueous solutions, where bitumen droplet spontaneously receded from the substrate (See Figure 3.6). [51] The whole process was recorded with high-speed camera under optical microscope (Zeiss Axiovert 200). The dynamic contact angles (i.e., the angle between the two tangent

lines at the TPC point) in the resulting images were analyzed with automated angle acquisition method; see Figure 3.7 for an example. [51]

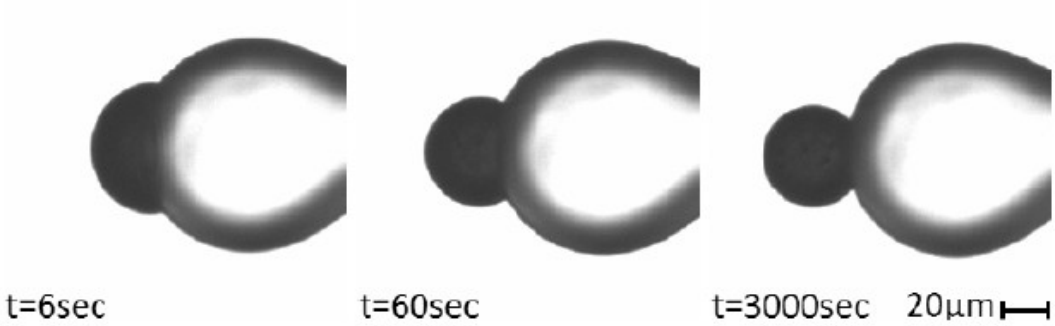

Figure 3.6: Typical images showing bitumen micro-droplet relaxation.[51]

In order to rule out other potential disturbing effect, vacuum distillation bitumen (VDU) provided by Syncrude Canada Ltd. and the stimulated process water (SPW) was used for all the contact angle measurements. The background electrolyte of the SPW contained 100 pm of $NaHCO_3$ and 500 ppm of NaCl as a buffer. The pH and the concentration of sodium ion in these electrolyte solutions were further adjusted to study the effect of NaCl on the static and dynamic contact angles at different values of aqueous pH.

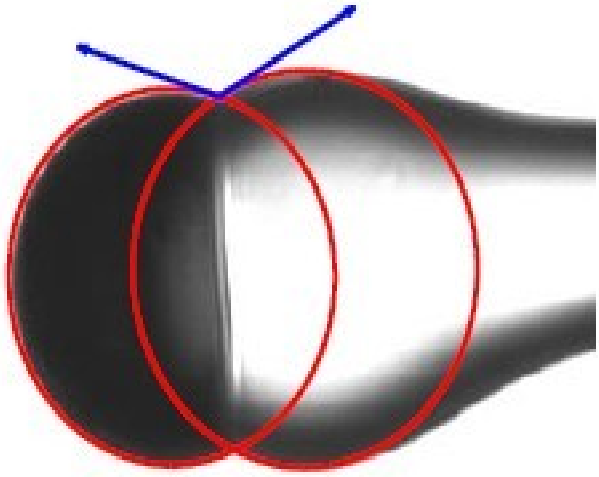

Figure 3.7: Schematics of determining contact angle using a shape fitting method.[51]

3.4.5 Induction Time Measurement

Induction time is defined as the contact time that can achieve 50% probability of attachment between an air bubble and bitumen surface.[52] To investigate the effect of sodium ions on bitumen aeration, a custom-built induction timer [37] was used. The vacuum-distillation-unit (VDU) feed bitumen was placed on a circular Teflon disk. The bitumen substrate surface was flattened by a razor blade. The bitumen sample was then immersed in the desired amount of water in a small rectangular glass cell. Before each test, bitumen sample was soaked in the water for around 30 minutes to reach equilibrium state. Additionally, in order to make the study similar to the real system, clay fines from the real oil sands deposit that was supplied by Teck Ltd. were used without any further treatment. To overcome the high turbidity and incapability of viewing the process of bitumen-air attachment in a suspension containing even as little as 0.5 wt% fines solids, sample of bitumen coated with these fines was prepared using the procedures as shown in Figure 3.8. Briefly, bitumen surface on the desk

being held by a tweezers and faced down toward the ground was conditioned in the fine suspension with slow agitation for 15 minutes. The fine-coated bitumen was then transferred to clear tailings water for the induction time measurement.

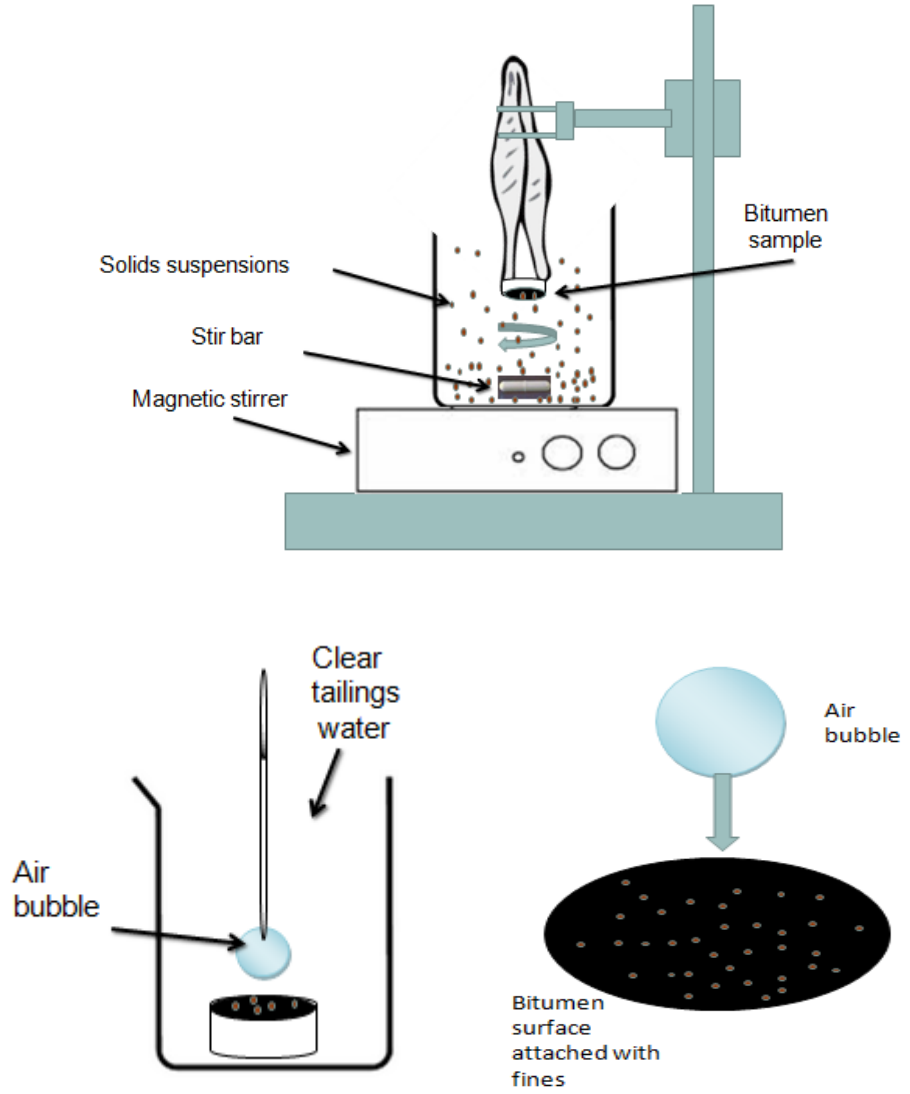

Figure 3.8: The procedure of preparing the sample of bitumen coated with fines.

The experimental setup of an induction timer is schematically shown in Figure 3.9. A three-axial micro translation state was used to hold the rectangular glass cell. Above the translation stage, one end of glass capillary tube was connected to a diaphragm of

speaker that was used to drive the tube approaching, holding and retracting to the bubble at accurate speed from bitumen surface through a charge amplifier controlled by a computer. For every approaching-holding-retracting cycle, the initial gap between the air bubble and the bitumen surface was set at 4 mm. The fresh air bubble generated with a micro syringe at the end of the capillary tube was 1.5 mm in diameter. With the help of the speaker diaphragm, the air bubble was controlled to approach the bitumen surface at a speed of 40 mm/s, make contact with the bitumen surface at preset contact time, and then retract at the same speed. The entire attachment process was recorded by a CCD camera equipped with a macro lens, and displayed on the computer. Sample cell was illuminated by a light source placed on both sides of the cell. For a particulate contact time, the contact was repeated for at least 20 times, the number of the attachment over the total contact time is defined as the probability of attachment at this certain attachment time. The probability of attachment as a function of the contact time was plotted, and was fitted with Boltzmann curve to obtain the time (i.e., induction time) required for the 50% probability of attachment. Temperature was measured by a J-type thermocouple and controlled by a portable heater. Unless otherwise stated, the temperature of water bath was kept constant at 50°C for all the induction time measurements that were identical to that of the above WBE.

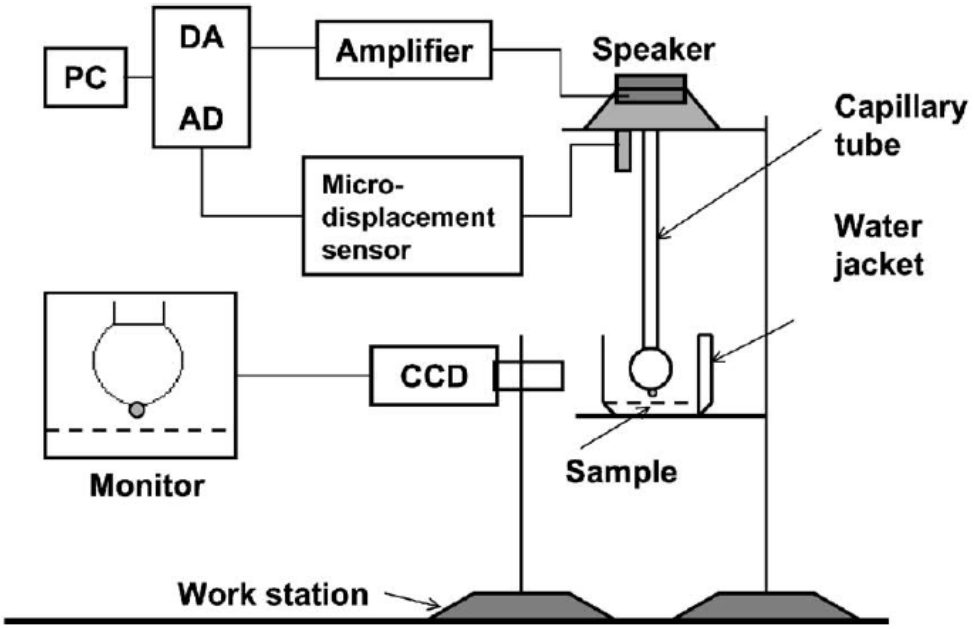

Figure 3.9: Schematics of induction timer setup.[37]

3.4.6 Zeta-potential Measurement

The zeta potential measurement was carried out with a Zeta PALS (Brookhaven) that uses the basic principle of phase-analysis of light scattering. In this study, for each sample the measurement was repeated at least ten times at room temperature. The fines suspension was prepared as follow: the fines separated from the froth in the above-mentioned flotation of the three different ores were mixed with tailings water of different sodium chloride concentration at a mass ratio of 1:1000. The suspension was then further diluted with tailings water to about 0.01 wt%, and dispersed by the ultrasonic dismembrator for 5 minutes. For the bitumen emulsion, the sample preparation also followed the same procedure using VDU bitumen.

Chapter 4: Results and Discussion*

4.1 Effect of Salinity on Bitumen Extraction

To understand the role of salinity on bitumen extraction, bitumen flotation tests were conducted using a laboratory-scale Denver flotation cell, initially at slurry pH 8.5 with the addition of different amount of sodium chloride (NaCl). The dosages of this salt were 0, 500, 1000, 2000 and 4000 ppm, based on the mass of the process water used for extraction. Oil sands ores of three different fines contents (low, medium and high) — denoted as Sun08, MA and AE 13 were tested and the extraction temperature was kept at 50°C. The averages of two repeated tests under the identical conditions are reported with errors. Note that pH 8.5 and temperature 50°C of process water are the current operating conditions of warm water-based bitumen extraction (WWBE) process widely used in the industrial practices.

Figure 4.1 shows the results of the primary and overall bitumen recovery of the three ores in the presence of various levels of sodium addition. It can be clearly seen that for the same salt dosage, both primary and overall bitumen recovery was deteriorated with increasing fines percentage in the solids of ores (or the decrease of the ore grade). For example, the primary bitumen recovery in the background process water (the symbols pointed to zero ppm of the added NaCl on the top figure of Figure 4.1) was approximately 84% for Sun08 containing very low percent of fines, in contrast to 27%

*: **This chapter is to be considered for a journal publication.**

and 20% of primary bitumen recovery for MA and AE13 ores that contained a medium and high amount of fines, respectively.

The most interesting observation in Figure 4.1 is that either primary or overall bitumen recovery for the same ore in response to the increased salinity was quite different, depending on the grade of the ore (or the fine amount in the ore solids). For the high-grade ore Sun08, both primary and overall bitumen recovery seemed to be insensitive to increasing the salt addition and remained satisfactory in the presence of up to 4000 ppm (i.e., the highest dosage in this study) of NaCl. However, for both medium- and low-grade MA and AE13 ores, the primary and overall bitumen recovery decreased with increasing sodium chloride addition — e.g., the overall recovery rate of AE13 dropped from 66% to 50% when the salt addition increased from 0 to 4000 ppm into the process water.

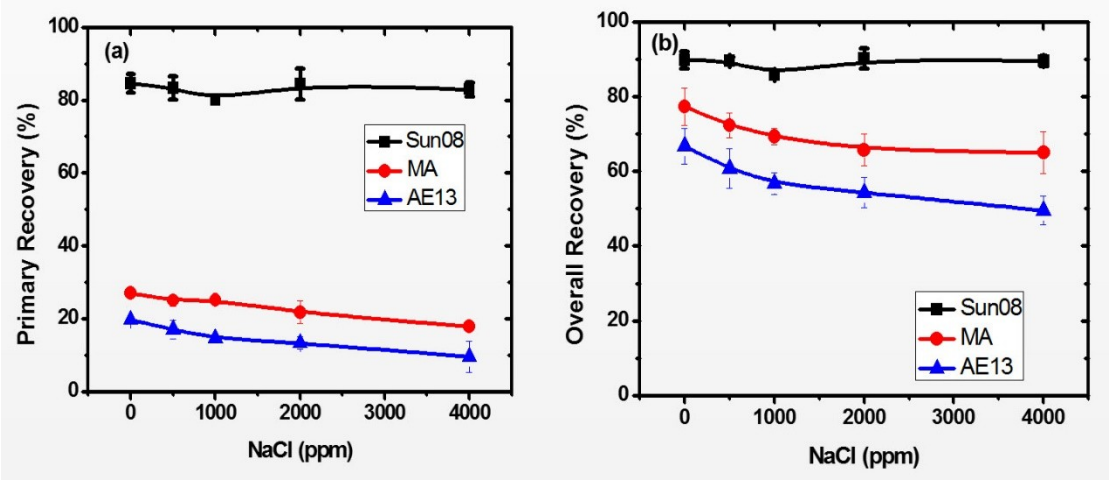

Figure 4.1: Effect of salinity on bitumen recovery from the three ores: (a) primary and (b) overall bitumen recovery.

The similar phenomena were observed for the bitumen froth quality. The results of the mass of bitumen, solids and water content in the primary and overall froth are shown in Figure 4.2 and Figure 4.3, respectively. The mass of bitumen relative to those of solids and water in the primary and overall froth extracted from the low-fines ore Sun08 was high and kept almost constant at different NaCl addition levels. For the froth generated from both medium- and high-fines ores, the absolute and relative amounts of bitumen were relatively low, and exhibited dropping with increasing salt dosage, although the extents of change were less significant than those of the salinity effect on bitumen recovery rate.

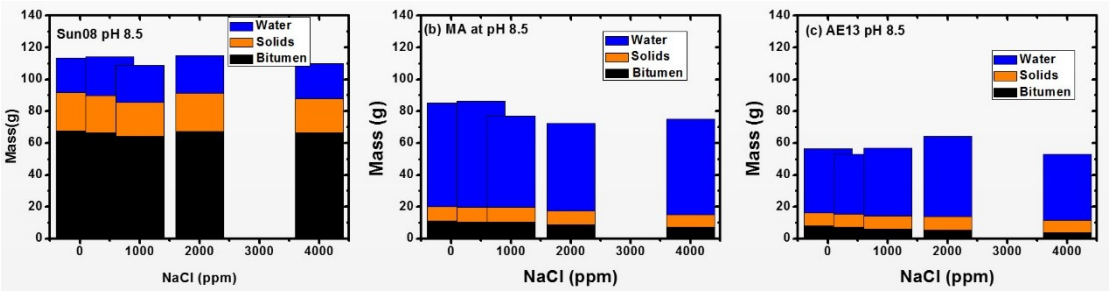

Figure 4.2: Effect of salinity on the mass of bitumen, solids and water in the primary froth: (a) Sun08, (b) MA (middle) and (c) AE13.

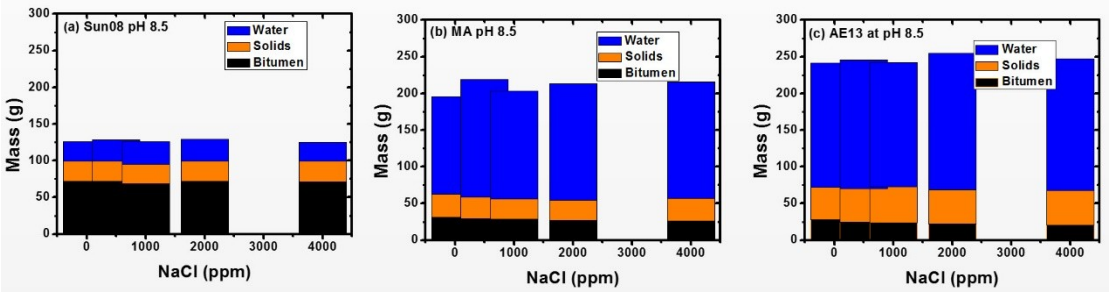

Figure 4.3: Effect of salinity on the mass of bitumen, solids and water in the overall froth: (a) Sun08, (b) MA, and (c) AE13.

For easy comparison, the bitumen to solids (B/S) ratio — a most significant parameter indicating the bitumen froth quality was calculated. The impact of salinity on B/S ratio of the primary and overall froth for the three ores is shown in Figure. 4.4. Again, the same trends are seen: The B/S ratio in the primary and overall bitumen froth of the high-grade ore Sun08 was relatively high and remained at 3.0 and 2.7, independent of the addition of the salt. In contrast, the B/S ratios of the froth from the MA and AE13 ores were low and showed a decreasing trend with increasing salt concentration for both primary and overall bitumen froth. Overall, it is revealed from the aforementioned extraction results of both the bitumen recovery and froth quality that the effect of increasing salinity was ore-dependent; higher salinity had a negligible impact on the processability of a high-grade ore, but showed a negative impact on the processing of medium- and low-grade ores.

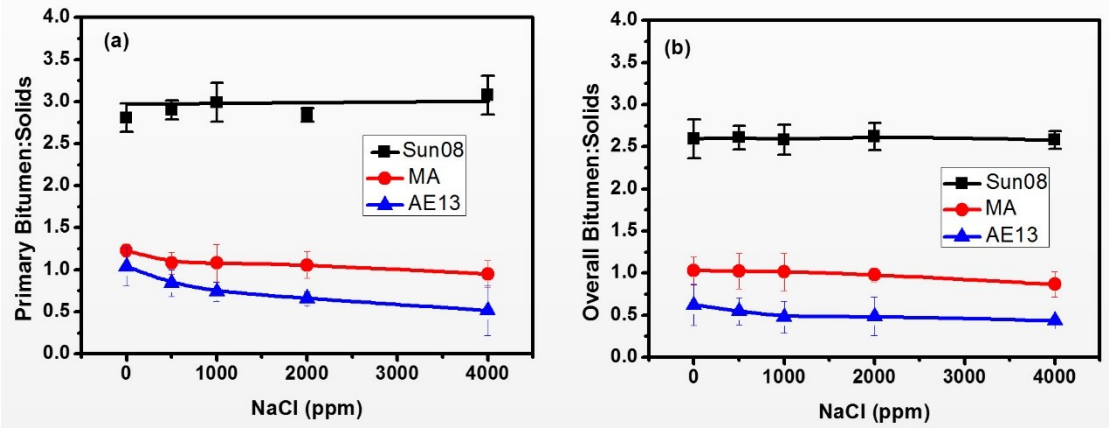

Figure 4.4: Effect of salinity on bitumen/solids ratio: (a) primary froth and (b) overall froth.

4.2 Working Mechanism of Salinity Impact

As mentioned earlier, it is widely recognized that the water-based bitumen extraction

(WBE) involved two essential steps — bitumen liberation and aeration. There has also been suggested that solid wettability and interaction between fines and bitumen play an important role in bitumen recovery. Therefore, it is significant to evaluate the role of salinity on these two fundamental aspects to explain the above-described ore dependence of salinity effect on the processability of oil sands.

4.2.1 Bitumen Liberation

The effect of salinity on bitumen liberation from the real oil sands ores was studied by the direct visualization method. Process water, with and without sodium chloride addition, of pH 8.5 was used (identical aqueous condition as used in the above bitumen flotation). The results of degree of bitumen liberation (DBL) as function of time are shown in Figure 4.5. When compared with the ultimate DBL (i.e., the DBL at the equilibrium state) of the three ores at the same salt dosage, the low fine Sun08 ore showed the relatively higher bitumen liberation, followed by the average MA and high fines AE13 ores. This result suggests that the presence of fines was detrimental to some degree to bitumen liberation. Interestingly, as for the sodium effect on the same ore, the results at aqueous pH 8.5 shown in Figure 4.5 revealed a negligible decrease in bitumen liberation kinetics (i.e., the rate of liberation to achieve an ultimate state) and a slightly lower ultimate DBL, regardless of the bitumen grade. For example, with no NaCl added, about 40% of bitumen liberated from the MA ore within 10s and the respective ultimate DBL was 54%. When 4000 ppm salt was dosed, 37.5% bitumen was liberated from MA within 10s, with 49.8% ultimate DBL. This

finding implies that the results of bitumen liberation were not able to reveal the ore-dependent impact of salinity on bitumen recovery and froth quality of medium- and low- grade ores at the normal extraction pH 8.5.

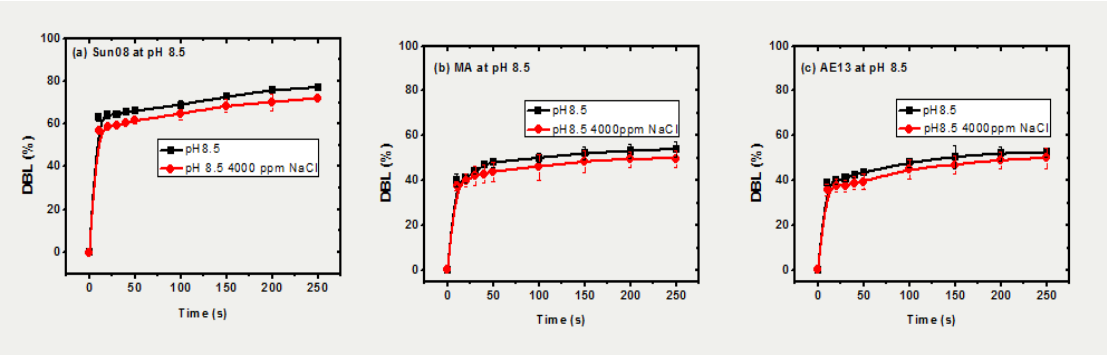

Figure 4.5: Effect of salinity on the degree of bitumen liberation (DBL) from the three ores at pH 8.5: (a) Sun08, (b) MA and (c) AE13.

4.2.2 Contact Angle Measurement

As a supplement to the liberation, bitumen recession from a model glass micro-sphere (similar to silica sand grain) was investigated in the presence of stimulated process water at pH 8.5 with two varied dosages of NaCl. As shown in the images of Figure 4.6, the contact line of bitumen retracted with time from the glass surface while the water was advancing until reaching an equilibrium configuration. It was observed that the velocity of contact line movement decreased with time as the bitumen retraction approaches the equilibrium state. Quantitatively, the resulting water-advancing contact angles as function of time could be measured and the results are shown in Figure 4.6. The rate of dynamic contact angle change is expressed by the initial slope of the curve. The steeper curve indicates a quicker recession of bitumen, while the

smaller equilibrium contact angle implies the easier detachment of bitumen from the solid surface. Similar to bitumen liberation results shown in Section 4.2.1, results in Figure 4.6 also show an insignificant effect of salinity on both dynamic and ultimate state of bitumen recession, as indicated by the two almost-overlapping contact angle profiles at two different salt addition levels.

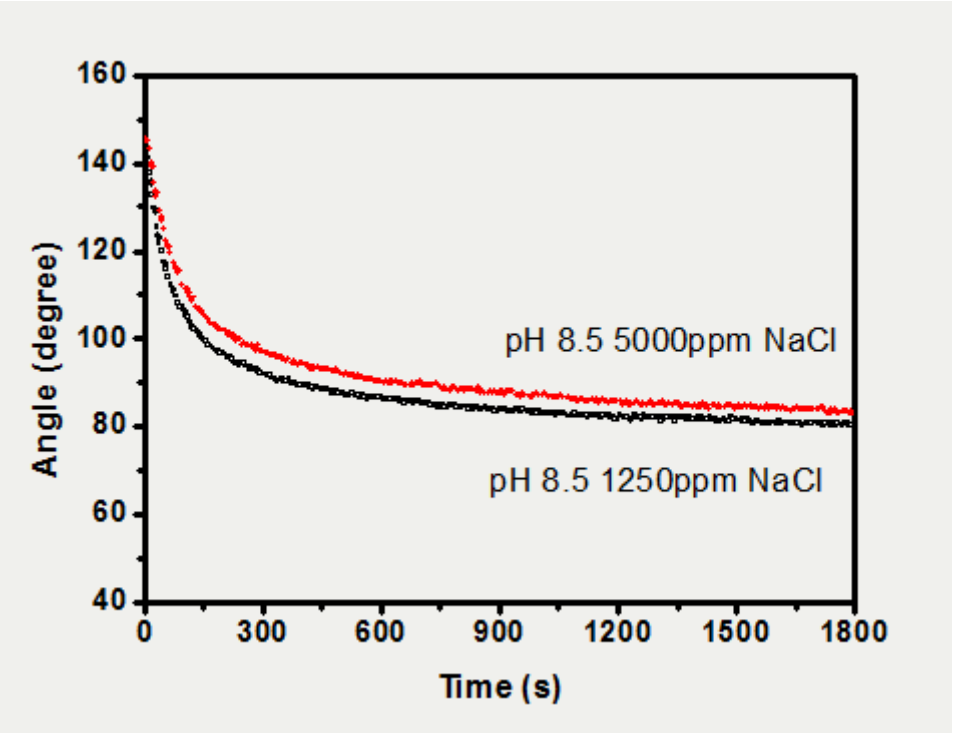

Figure 4.6: Effect of salinity on the dynamic and static contact angles of bitumen recession from a glass microsphere in simulated process water at pH 8.5.

4.2.3 Induction Time of Bitumen Aeration

To evaluate the effect of increasing sodium concentration on bitumen aeration, the probability of air bubble-bitumen attachment with and without fines slime coating as a function of their contact time was measured in the process water at pH 8.5 and 50^{o}C. The measured probability of attachment is plotted as a function of contact time as

shown in Fig 4.7. From these curves, the respective induction time was obtained as the contact time of 50% probability of attachment as demonstrated in Figure 4.8. It is obvious that in case of fine solids, it took a shorter contact time to achieve the same (e.g., 50%) probability of bitumen-air bubble attachment in the presence of 4000 ppm NaCl addition than the case without salt addition to the process water, indicating a decrease in induction time of bitumen-air bubble (no fine) attachment with increasing salt dosage. The most plausible reason for the observed decrease in the induction time with increasing salt concentration is the compression of the electric double layers around the bitumen and air bubbles in aqueous solutions of increasing sodium ion concentrations. As a result, the electrostatic repulsions between air bubble and bitumen would be reduced, leading to an enhanced drainage and rupture of thin water films between bitumen and air bubbles during the attachment process, as illustrated in the left-hand side of Figure 4.9.

The fines-coated bitumen was prepared by soaking the VDU bitumen in the tailing water containing 0.5 wt% clay fines. Fines deposited on the bitumen surface, thus the wettability of bitumen surface would be altered from an oil-wet (favorable to attachment to the hydrophobic air bubbles) to a less oil-wet (or more water-wet) characteristics. The more the fines are coated on the bitumen surface, the more water-wet it would be. Increasing the salinity of water decreases EDL repulsion between the fines and bitumen as mentioned earlier. As a result, more fines are anticipated to be deposited onto the bitumen surface, resulting in an increased

resistance to the formation of three phase contact of bitumen, water and air bubble, [37] as shown in the right-hand illustration of Figure 4.9. In other words, increasing salt dosage (from 0 ppm to 4000ppm) created a detrimental condition for the bitumen and air bubble attachment in the presence of fines, as indicated by the higher induction time of fines-coated bitumen and air bubble attachment, shown in Figure 4.8. Considering that the fines-coating of bitumen requires the presence of fines in the system, it is anticipated that the lower the grade of the oil sand ore, the higher the probability of fines slime coating on the bitumen surface, making the bitumen aeration more difficult. In this aspect, the negative effect of salinity on the bitumen and air bubble attachment in the presence of fines would be the most responsible for the ore-dependent nature of salinity impact on the processing of mineable oil sands, explaining the observed reduction of bitumen recovery and froth quality for the medium-fines MA and the high-fines AE13 ores.

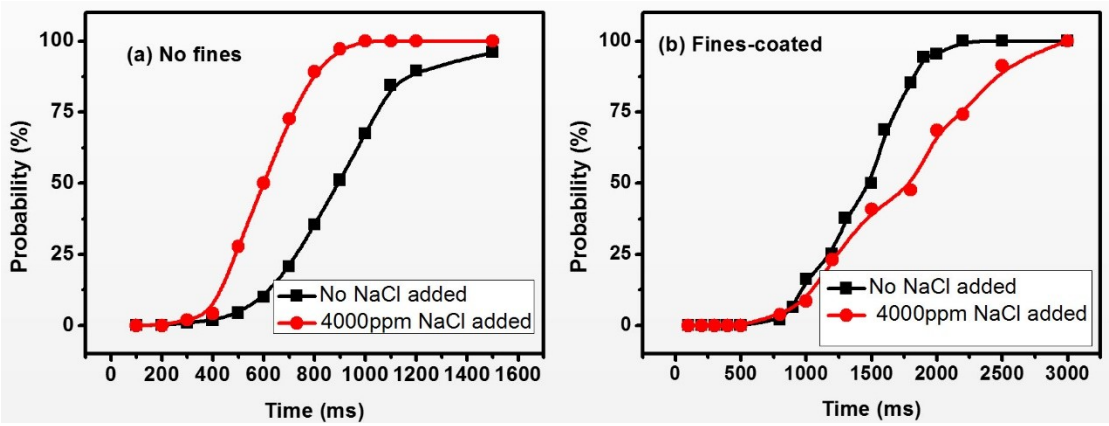

Figure 4.7: Effect of salinity on probability of air bubble attachment with: (a) bare bitumen and (b) fines-coated bitumen.

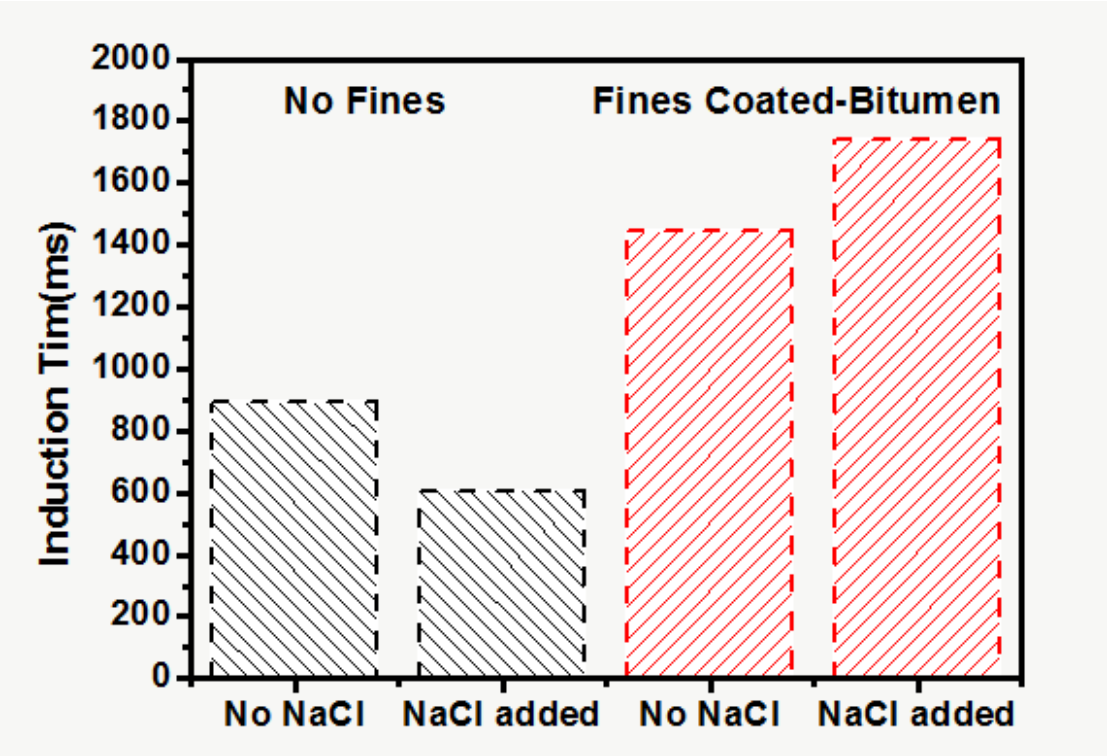

Figure 4.8: Effect of clay fines on bitumen and air bubble attachment.

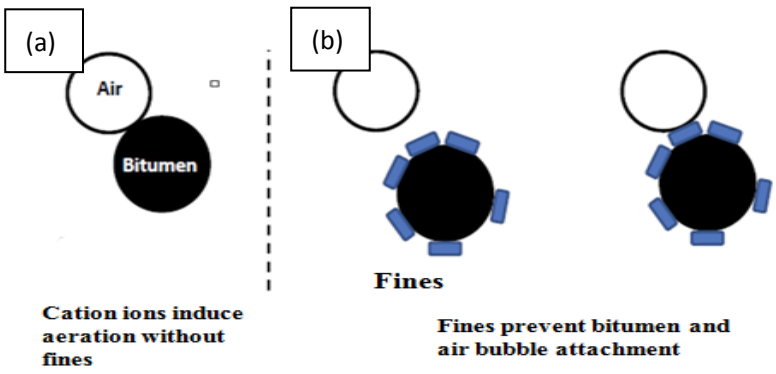

Figure 4.9: Illustration of bitumen and air bubble attachment (a) without fines and (b) with fines.

4.2.4 Zeta Potentials of Suspended Fines and Bitumen

Doping a significant amount of sodium ions is known to affect the ionic strength and

hence the Debye length of the solution. As a result, the interfacial properties including the surface charges of suspended particles or droplets are anticipated to change. In order to study how the sodium ions affect the surface charges on solids and bitumen, the zeta potential of suspended fines from the froth of bitumen extraction and bitumen emulsions in the tailings water at pH 8.5 was measured. The results are shown in Figure 4.10.

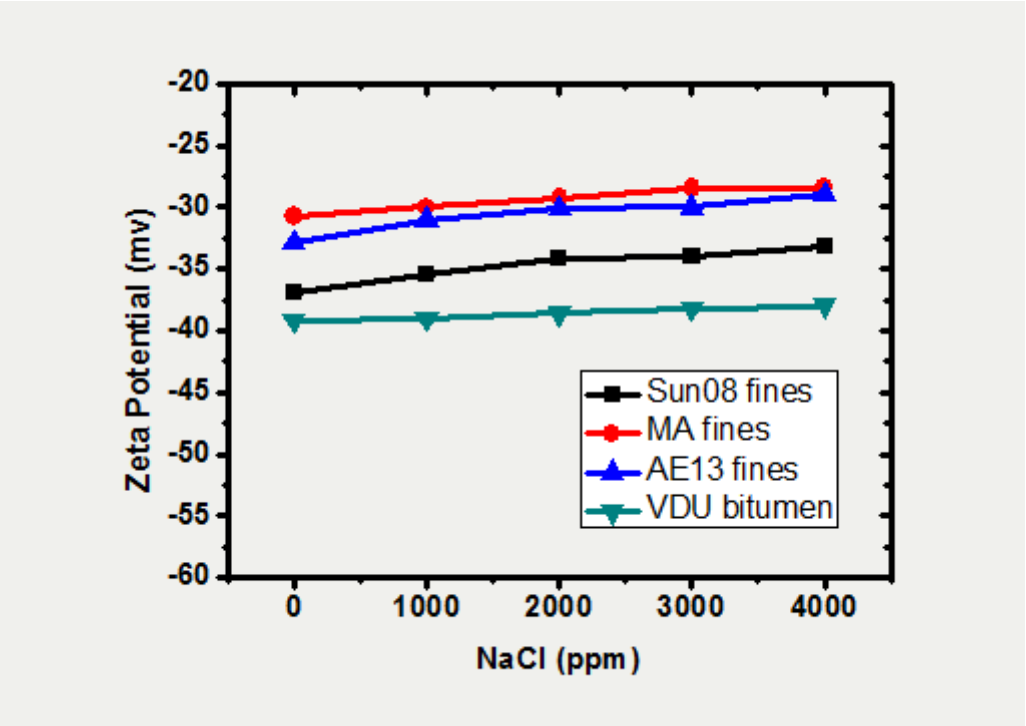

Figure 4.10: Zeta potentials of suspended fines (taken from the froth) and VDU bitumen in clear tailings water at pH = 8.5.

It is not surprising to see from the data in Figure 4.10 that in aqueous solutions containing any amount of Na^+ at pH 8.5, the bitumen and fines from these three ores were all negatively charged. With increasing Na^+ concentration, the zeta potentials curves for the fines of froth from the three ores became slightly less negative, so were

the bitumen in water emulsions. For example, the zeta potentials of the fines from Sun08 froth and bitumen were increased from -36.9 mV to -33.2 mV and from -39.17 mV to -38.01 mV, respectively, as the sodium chloride concentration increased from 0 to 4000 ppm. These results suggest that Na^+ ion was not a potential-determining ion or specific adsorbing ion. However, the zeta potentials of the fines were dependent on the source of oil sands ores from which the froth fines were obtained. The zeta potential of the respective fines (from the froth of high-grade Sun08 to low-grade AE13 ores) appears to be less negative with decreasing the grade or increasing the fines content of ores. Since the surface of bitumen were also negatively charged and assuming the same zeta potentials of bitumen emulsions from all the sources, the interactions of fines-bitumen would therefore be less repulsive for the AE13 and MA ores than for the Sun08 ore. This finding is likely one of possible factors contributing to the decreased bitumen recovery and the poorer froth quality of processing AE13 and MA ores than Sun08 ore.

4.3 Remediation via Caustic Addition: a Strategy of Failure

It was demonstrated in the previous section that the increasing salinity had a negligible effect on the warm water-based bitumen extraction (WWBE) of a good-grade ore, but was detrimental to the medium- and low-processability ores. With the eventual decline of high-quality oil sands deposits, processing of relatively poor-quality ores will be inevitably on the rise in the foreseeable future. In order to counterbalance the negative effect of increasing salinity, developing a remediation

strategy is a clear necessity. One conventional practice in oil sands industry to improve the bitumen recovery from relatively poor-processing ores is via caustic, mainly sodium hydroxyl addition, i.e., extraction at higher aqueous pH. The lower the grade of the ore to be processed, the higher of the caustic dosage will be used. In this study, the application of caustic was used to evaluate whether the caustic addition could alleviate the negative effect of high salinity on flotation of poor-processing MA and AE13 ores.

4.3.1 Effect of salinity on bitumen flotation at increased pH

A series of flotation tests using the same procedure declared in Sections 3.4.1 and 4.1 were conducted for the three ores in varied sodium addition levels to the process water at pH 11.2. The results of primary and overall bitumen recovery are shown in Figure 4.11. At this pH (pH 11.2), the effect of increasing salt dosage was also shown to be ore-dependent. But surprisingly, the bitumen recovery of medium (MA) and high (AE13) fines ores suffered a larger loss at the same amount of NaCl added when processed at pH 11.2 than at pH 8.5. For example, as the sodium chloride addition level increased from 0 to 4000 ppm, bitumen recovery for medium and high fines ores dropped at pH 11.2 from 76% to 53% and 65% to 40%, respectively. In contrast, the bitumen recovery decreased from 77% to 65% and 66% to 50% for the medium and high fines ores at pH 8.5 when 4000 ppm sodium chloride was added.

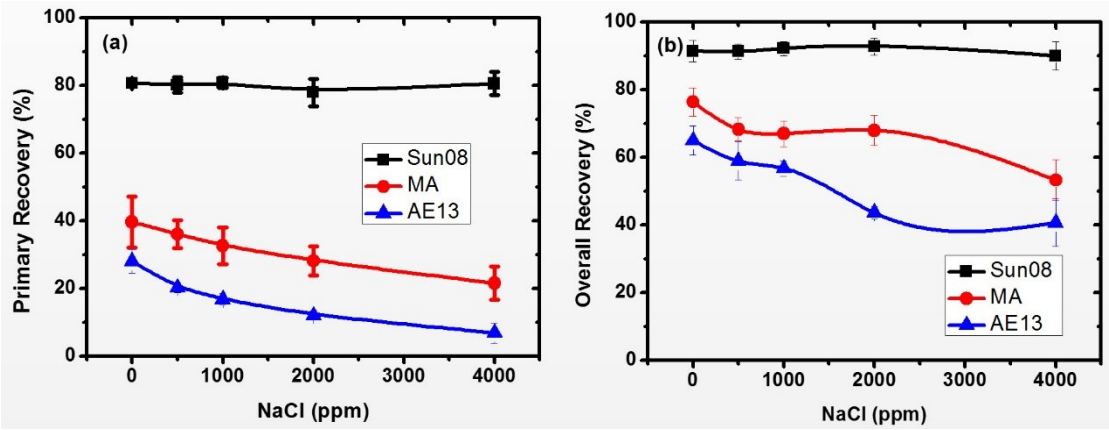

Figure 4.11: Effect of salinity on (a) primary recovery and (b) overall recovery of bitumen from three ores in the process water at pH 11.2.

The similar depression with increasing salt concentration on bitumen froth quality in terms of bitumen over solids (B/S) ratio was observed for both primary and overall froth from MA and AE13 ores as shown in Figure 4.12. Despite the better froth quality at pH 11.2 than at pH 8.5 (likely contributed to the increased electrostatic repulsive force at higher pH), the change of B/S ratio at pH 11.2 was much steeper than at pH 8.5. Clearly, higher pH made the negative effect of adding 4000 ppm NaCl on froth quality in terms of the B/S ratio worse, suggesting that increasing pH was not able to solve but exaggerated the negativity effect of sodium ions. Takamura et al. [56] also confirmed that Na^+ up to 1725 ppm could reduce as much as 45% bitumen recovery, and the negativity of sodium effect on bitumen recovery was even larger at higher pH.

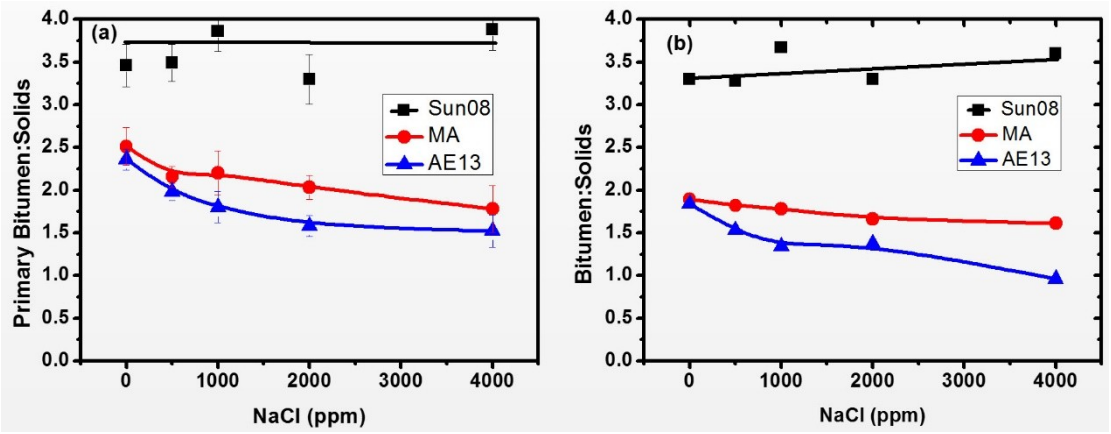

Figure 4.12: Effect of salinity on (a) primary and (b) overall bitumen/solids ratio of the froth extracted from three ores in the process water at pH 11.2.

To explain the failure of using caustic to alleviate the negative effect of increasing salinity on oil sands extraction, the effect of the salt addition on bitumen liberation from the three ores, bitumen recession (dynamic and static contact angles) from model glass microsphere, induction time of bitumen-air bubble attachment, and zeta potentials of the froth fines and VDU bitumen suspension was studied at pH 11.2.

4.3.2 Effect of salinity on bitumen liberation at more alkaline pH

High salt concentration in the industrial process water is thought pernicious to bitumen liberation, probably due to the reduction of electrostatic repulsive force between bitumen and sand grains.[41,42] Another possible explanation is that the production of natural surfactants is hindered by increasing sodium concentration, giving rising to poorer bitumen liberation.[27] The results of the degree of bitumen liberation (DBL) for the three oil sands ores in the process water of pH 11.2 at two sodium chloride addition levels are shown in Figure 4.13. A more dramatic depression

of the DBL occurred for all the three ores. The ultimate DBL decreased from 72% to 41%, 60% to 52%, and 56% to 49% for Sun08 (low fine), MA (medium fine) and AE13 (high fine) ore, respectively. In comparison, the ultimate DBL at pH 8.5 decreased only slightly from 57% to 52%, 52% to 50%, and 52.6% to 50% for Sun08, MA and AE13 ores, respectively as shown earlier, indicating an increased negative effect of salinity on bitumen liberation with increasing pH.

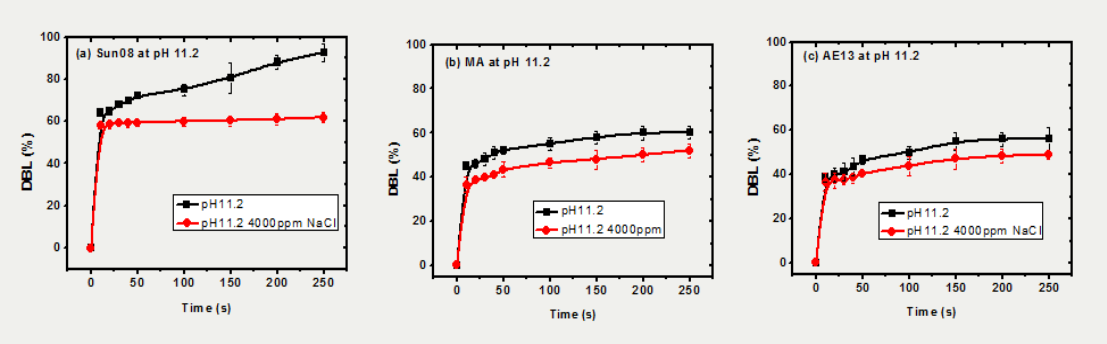

Figure 4.13: Effect of salinity on the degree of bitumen liberation (DBL) from the (a) Sun08, (b) MA and (c) AE13 ores in the water at pH 11.2.

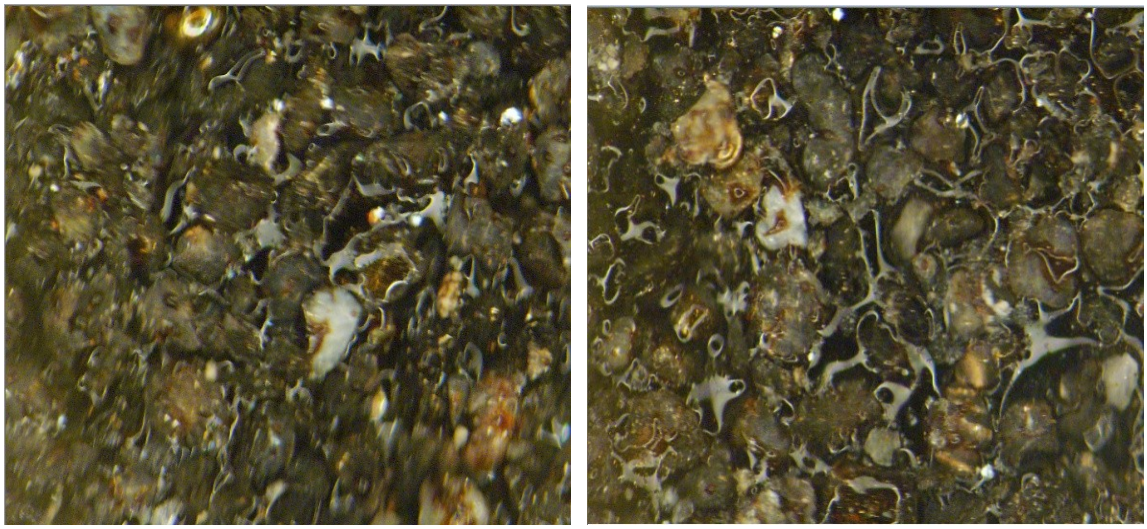

(a) (b)

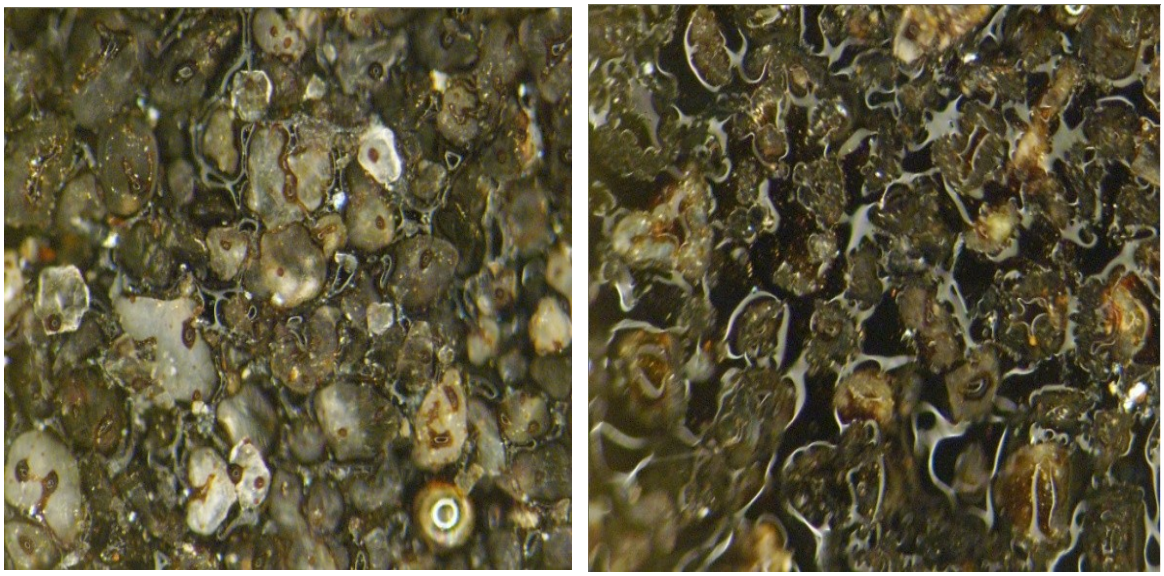

(c) (d)

Figure 4.14: Images of bitumen liberation for Sun08; (a) at pH 8.5 without NaCl added; (b) at pH 8.5 with 4000 ppm NaCl added; (c) at pH 11.2 without NaCl added; and (d) at pH 11.2 with 4000 ppm NaCl added.

4.3.3 Effect of salinity on bitumen recession at more alkaline pH

Again, as a confirmation, bitumen recession dynamics from a close-ended spherical glass micropipette was determined in the stimulated process water at pH 11.2 and two different sodium ions concentrations. Similar to the results of bitumen liberation, the effect sodium addition on the equilibrium contact angle was more significant at higher pH of 11.2 than at lower pH of 8.5. The equilibrium contact angle measured from the aqueous phase increased from 45° to 57° (i.e., less water-wet) when the sodium ion concentration increased from 500 ppm to 2000 ppm at pH 11.2, larger than the value at pH 8.5 with the same dosages of the salt. This result was consistent with the results of previous contact angle measurement by Basu et al. [26] who showed a more

pronounced effect of NaCl on the contact angle at higher pH.

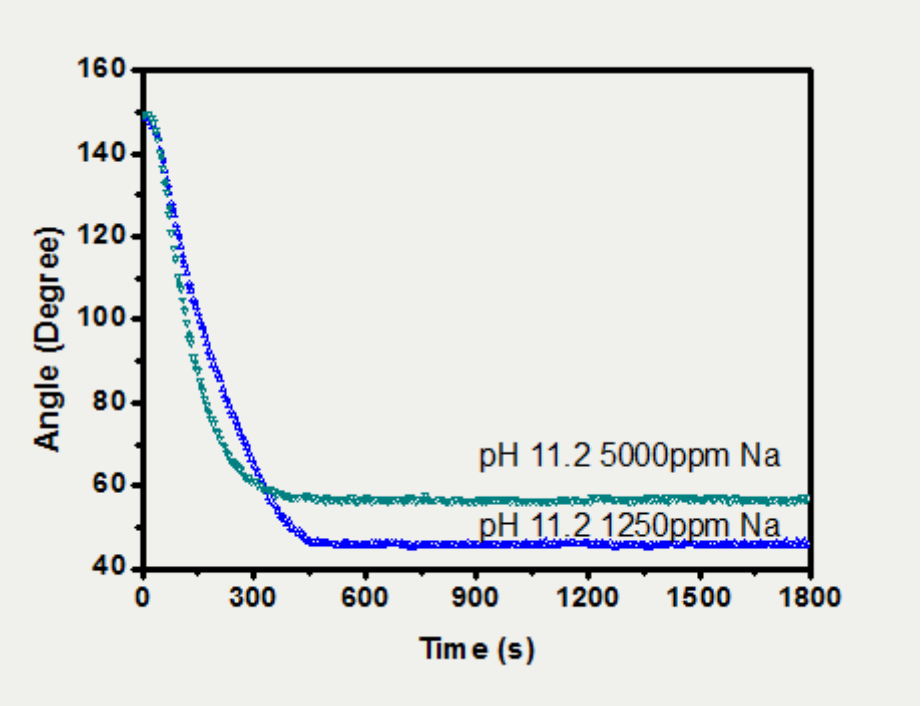

Figure 4.15: Effect of salinity on dynamic and static contact angles of bitumen recession from a glass microsphere in simulated process water at pH 11.2.

4.3.4 Effect of salinity on bitumen aeration at more alkaline pH

Induction time measurement of bitumen-air bubble attachment was conducted at pH 11.2 with two varied salt concentrations in the presence of clay fines. The probability of attachment vs contact time curve and the induction time are presented in Figure 4.16. The same trend as observed at pH 8.5 was seen. Sodium ions induced slime coating on bitumen, and prevented bitumen-air bubble attachment. Compared with the induction time measurement in the presence of fines at two pHs (see Figure 4.16), the difference was 293 ms at pH 8.5 while the difference was 494 ms at pH 11.2. This contrast difference indicates that the bitumen surface was easier to be affected by the increased salinity at higher pH, so that a larger amount of fines could be attached to

the bitumen surface, forming a solids layer to prevent the attachment of bitumen to the air bubbles.

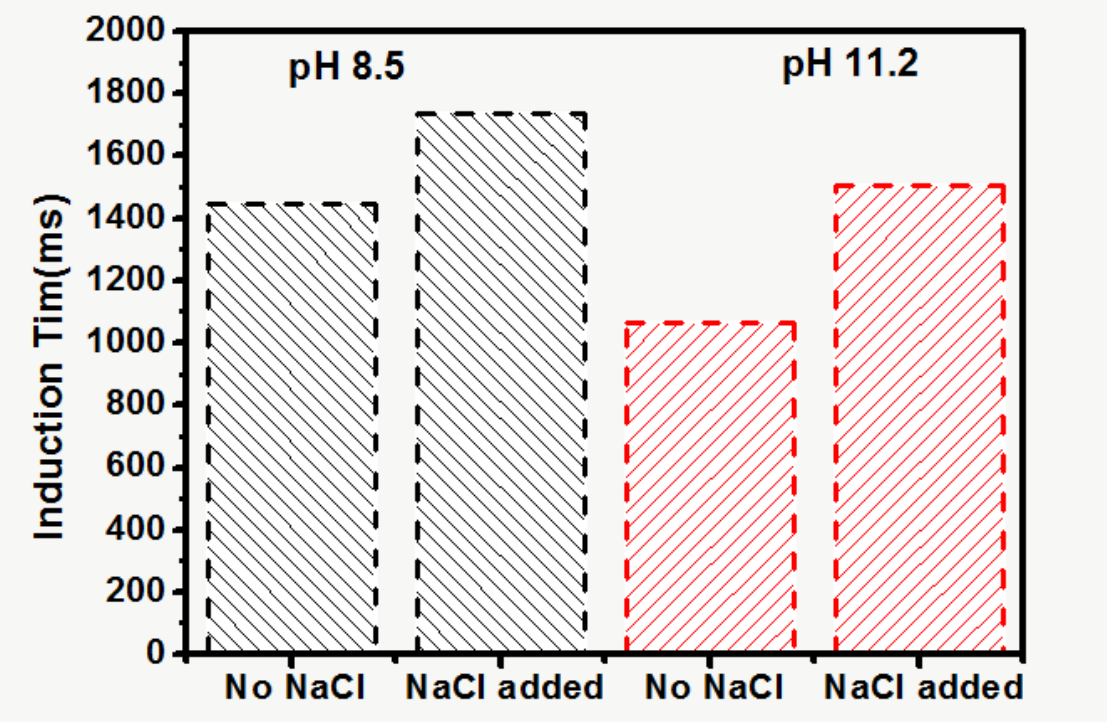

Figure 4.16: Effect of salinity on induction time of bitumen-air bubble attachment (aeration) at pH 8.5 and pH 11.2 with fines addition.

4.3.5 Effect of salinity on zeta-potential at more alkaline pH

Zeta potential data at pH 11.2 are presented in Figure 4.17. The zeta potentials of bitumen emulsions and froth fines were more negative at pH 11.2 than at pH 8.5, indicating an increased adsorption of natural surfactant and ionization of silicon hydroxide at bitumen water and solids-water interfaces, respectively [31]. However, when salinity was increased with NaCl addition, the zeta potential increased sharply for all samples. Due to the higher negative charge density on the interfaces, sodium

ions are easier to access and adsorb on the bitumen-water or solids-water surface. The greater change of zeta potential with sodium ion addition at higher pH for both bitumen and froth fines explains well the results of bitumen liberation, bitumen recession on glass tip, and bitumen-air bubble attachment. The more significant effect of sodium ion addition at higher pH on these interfacial phenomena resulted in a more significant decrease in bitumen recovery and froth quality for medium and high fine ores, indicating that increasing pH cannot alleviate the negative effect of sodium ion accumulation in process water on bitumen extraction.

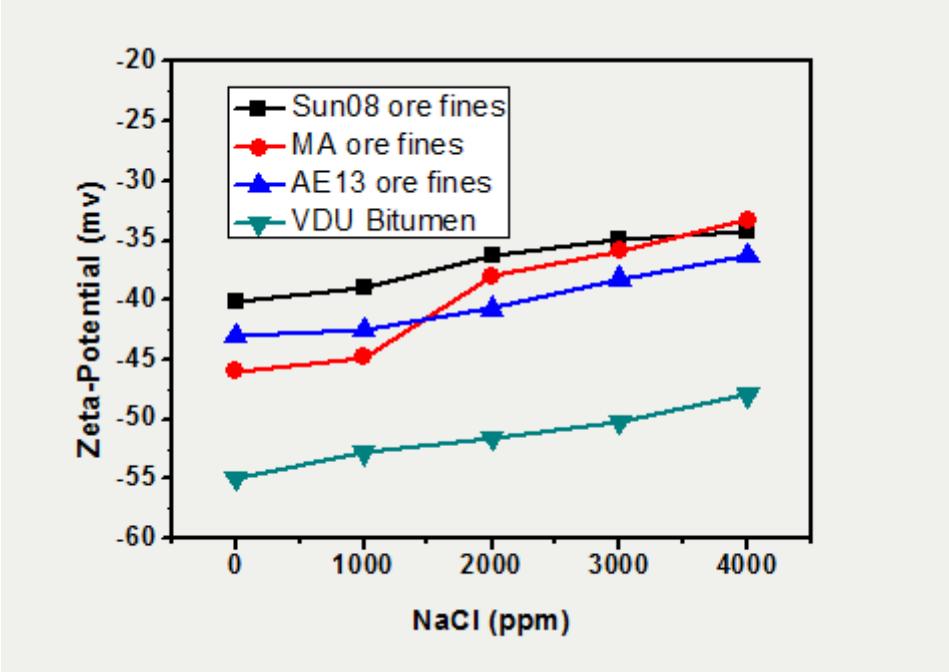

Figure 4.17: Effect of salinity on zeta potential of oil sands fines and VDU bitumen in the tailings water.

4.3.6 Discussion

It is known that higher sodium concentration leads to a poorer bitumen recovery and froth quality for the medium and poor processing ores. Liberation study showed that higher electrolyte concentration hinders the separation of bitumen from sand grains.

Unlike the calcium ions, which consume certain amount of surfactant in the aqueous solution and therefore increase bitumen and water interfacial tension, higher sodium ions decreased the bitumen-water interfacial tension. [1] Heimenz [53] and Cai[54] also confirmed that the interfacial tension of a pure hydrocarbon decreased with increasing the salinity of aqueous solutions when a small amount of surfactant is present.

Han et al. [55] proposed that the solid-liquid specific free energy can be consisted to consist of two parts:

$$\gamma_{SW} = \gamma^{o}_{SW} + \Delta F_{dl} \qquad (4.6.6.1)$$

where γ^{o}_{SW} represents the solid-water interfacial tension at point of zero charge, while ΔF_{dl} is defined as the formation free energy of the ionizable surface relative to the point of zero charge. [55] At a low and constant surface potential, ΔF_{dl} is related to the surface potential by:

$$\Delta F_{dl} = -\ 1/2 \epsilon \epsilon_o \kappa \psi_o^2 \qquad (4.6.6.2)$$

where ϵ is the dielectric constant, ϵ_o is the permittivity of free space, κ represents the Debye length, and ψ_o is the surface potential.

At pH 8.5, adding sodium chloride into the system reduces the Debye length, compressing more on the electric double layer and hence increasing the interfacial tension of both solids and water. However, the change of zeta-potential as measured was negligible. Therefore, the increase in the solid-water interfacial tension is rather small. As a result, both the liberation test and contact angle measurement showed a

small depressing effect of sodium ion addition on bitumen recession. When the pH increased to pH 11.2, the effect of sodium ion addition is quite different. The bitumen-water interfacial tension was anticipated to decrease, but only a smaller change was observed at pH 11.2 than at pH 8.5. This smaller change in the interfacial tension at pH 11.2 is attributed to its lower original interfacial tension, as such that increasing sodium ion concentration could only lead to a limited further decrease in bitumen-water interfacial tension. For the solids, the decrease in Debye length with increasing sodium ion concentration increased the zeta potential of solids dramatically (from -43 mV to -34-mV as an average change for the three types of fines) as anticipated. As a consequence, the solids-water interfacial tension gained a large increase, leading to a more pronounced spreading of bitumen on solids surfaces. The results collectively explain why the sodium effect is more pronounced at higher pH of 11.2 than at relatively lower pH of 8.5.

4.4 Positive Strategy — Blending of Different-Grade Ores

To find a possible solution by considering a negligible effect of sodium ion concentration on processing of high grade ore, blending experiments were carried out using Sun08 (high grade and low-fines ore) and AE13 (low-grade and high-fines ore) at pH 8.5 with 4000 ppm NaCl added. Comparing the real recovery with the calculated additive recovery, the results in Figure 4.18 showed clear benefit of blending the ores at Sun08/AE13 greater than 1 for the primary recovery. Note that the calculated recovery is based on the individual floatation data of two different ores

(Sun08 and AE13). Unlike the primary recovery, blending showed a significant gain at any mass ratio of two ores. Similar advantages of blending oil sands have been reported by Takamura et al.[56] and Schramm et al.[57] In this situation, the loss of bitumen recovery for the high-fines ore was compensated by the addition of high-grade ore. Possibly, the increased bitumen to fines ratio alleviate the negative effect of sodium ion addition, as sodium ion addition showed a negligible influence on processing the high-grade ore. The mechanism of the observed enhancement in processability by ore blending needs further investigation.

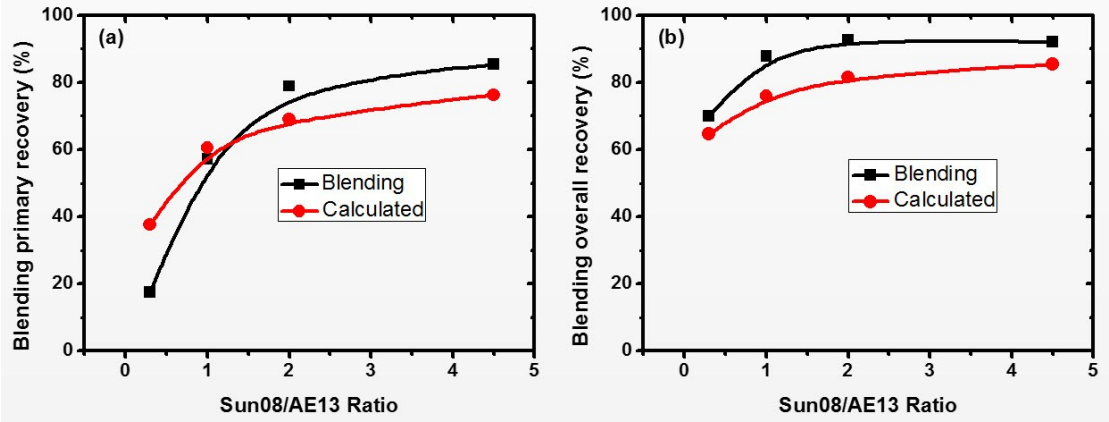

Figure 4.18: (a) Primary and (b) overall recovery from blends of high grade Sun08 and low-grade AE13 ores processed at pH 8.5 in the presence of 4000ppm NaCl.

Chapter 5: Conclusions

In this study, three types of oil sands ores were used to investigate the effect of salinity on processability of oil sands ores. The bitumen flotation tests were conducted in conjunction with the study of bitumen liberation and attachment to air bubbles (bitumen aeration). The effect of salinity on the bitumen recovery and froth quality was shown to be ore-dependent. Sodium chloride addition did not change the bitumen recovery from the high-grade ore at different pHs greater than 8.5. In contrast, increasing sodium concentration was shown to reduce the bitumen recovery and froth quality for the medium- and high-fine ores, mainly due to the less efficient bitumen-air bubble attachment. Increasing pH to 11.2, however, cannot alleviate the negativity effect of sodium ion addition on bitumen recovery and froth quality for the medium- and high-fine ores, instead it made the situation even worse. The results of examining the bitumen liberation and aeration processes supported the floatation data well at pH 11.2. A striking contrast of sodium ion effect on bitumen liberation and aeration was observed. Compared with the data at pH 8.5, more severe negative influence of 4000 ppm NaCl addition was observed on bitumen liberation at pH 11.2 for three types of ores. In addition, the influence of sodium ions on aeration at higher pH was also more noticeable, although the induction time was shorter than at lower pH. A more distinct the effect of sodium ion at higher pH on bitumen recession on glass microsphere in the simulated process water was also confirmed. The zeta potential measurement revealed that sodium ions depressed the electric double layer of bitumen emulsions and fines, making the zeta potentials of bitumen emulsions and

fines less negatively charged. At higher pH, the bitumen and fines surfaces were more negatively charged, making sodium ions easier to absorb and alter their surfaces properties. Finally, ore blending seems to be a promising choice of relieving the effect of sodium ion accumulation in process water.

References:

1. Masliyah, J.; Xu, Z.; Czarnecki, J. Handbook on Theory and Practice of Bitumen Recovery from Athabasca Oil Sands, Vol. I: Theoretical Basis; Kingsley Knowledge Publishing: Canada, **2011**.
2. Takamura, K. Microscopic Structure of Athabasca Oil Sand. J. Can. Chem. Eng. **1982**, 60(4), 538-545.
3. Energy Resources Conservation Board (ERCB). Alberta's Energy Reserves 2010 and Supply and Demand.
4. Masliyah, J., Zhou, Z., Xu, Z., Czarnecki, J., Hamza, H. Can. J. Chem. Eng. **2004**,82, 628–654.
5. Masliyah, J.M.; Gray, M.R. Extracting and Upgrading of Oilsands Bitumen. Course Pack. University of Alberta. **2011**.
6. Oil Sands Today website. www.oilsandstoday.ca/whatareoilsands/Pages/RecoveringtheOil.aspx
7. ERCB. Total E&P Canada Ltd. Surface Steam Release of May 18, 2006. Joslyn Creek SAGD Thermal Operation. ERCB Staff Review and Analysis Report. ERCB website. www.ercb.ca
8. Wikipedia website. www.en.wikipedia.org/wiki/Tailings
9. Government of Alberta. Fact Sheet: Alberta's Oil Sands-Tailings Management. August **2010**.
10. PEMBINA website. www.pembina.org/oil-sands/os101/tailings
11. Xu, Y., Cymerman, G. Flocculation of fine oil sand tails. Polymer in Mineral

Processing, Proceedings of the UBC-McGill Bi-Annual International Symposium on Fundamentals of Mineral Processing, 3rdu, Quebec City, QC, Canada, **1990**,591-604.

12. Mpofu, P., Addai, J., Ralston, J. Flocculation and dewatering behavior of smectite dispersions: effect of polymer structure Type. Miner. Eng. **2004**, 17(3), 411-423.
13. Sworska, A., Laskowski, J.S., Cymerman, G. Flocculation of the Syncrude fine tailings part 1: effect of pH, polymer dosage and Mg^{2+} and Ca^{2+} cations. Int. J. Miner. Process. **2000**, 60(2), 143-152.
14. Margo C. A Novel Flocculant for Enhanced Dewatering of Oil Sands Tailings. MSc thesis, University of Alberta. **2011**.
15. Erik. W. A. Process water treatment in Canada's oil sands industry: I. Target pollutants and treatment objectives. J. Environ. Eng. Sci. **2008**, 7: 123-138.
16. Qian Z. Understanding the Role of Caustic Addition in Oil Sands Processing. MSc thesis, University of Alberta. **2013**.
17. Hunter, J. Foundations of Colloid Science; Oxford University press: New York, **2001**.
18. Freundlich H. Colloid & Capillary Chemistry; Methuen publishing: London, **1926**.
19. Butt, J., Graf, K., Kappl, M. Physics and Chemistry of Interfaces. Wiley-VCH: Weinheim, **2003**.
20. Stern, O. The theory of the electric double layer. Z. Electrochem. **1924**, 30, 508.
21. Lin, W., et al. Sub-20nm node photomask cleaning enhanced by controlling zeta

potential. Website: http://spie.org/x91382.xml

22. Kumar, B., Crittenden., S. Stern Potential and Debye Length Measurements in Dilute Ionic Solutions with Electrostatic Force Microscopy. Nanotechnol. **2013**, 24, 435-701.
23. He., L. Mechanistic Study on Solvent Enhanced Bitumen Liberation from Oil Sand Ores. NSERC student presentation **2014.**
24. Basu,S., Nandakumar, K., Masliyah., J. A Study of Oil Displacement on Model Surfaces. J. Colloid Interf. Sci. **1996**, 182, 82-94.
25. Leja, J., Bowman., W. Application of Thermodynamics to the Athabasca Tar Sands. J. Can. Chem. Eng. **1968**, 46, 479-481.
26. Basu, S., Nandakumar, K., Masliyah, J. Effect of NaCl and MIBC/kerosene on Bitumen Displacement by Water on a Glass Surface. Colloids Surfaces A: Physicochemical and Engineering Aspects **1998**, 136, 71-80.
27. Sundeep, S., Chris. F., Artin, A., Masliyah, J. Study of Bitumen Liberation from Oil Sands Ores by Online Visualization Energy Fuels **2012**, 26, 2883-2890.
28. Liu, J., Xu, Z., Masliyah, J. Studies on Bitumen-Silica Interaction in Aqueous Solutions by Atomic Force Microscopy. Langmuir **2003**, 19, 3911-3920.
29. Zhao, H., Dang-Vu, T., Long, J., Xu, Z., Masliyah, J. Role of Bicarbonate Ions in Oil Sands Extraction Systems with A Poor Processing Pre. J. Dispersion Sci. Technol. **2009**, 30,809-882.
30. Israelachvili, N. In Intermolecular and surface forces; Academic Press: **1991**.
31. Nguyen, A.; Schulze, J. In Colloidal science of flotation; surfactant science series;

New York, **2004**.

32. Mao, L.; Yoon, R. Predicting Flotation Rates using a Rate Equation Derived from First Principles. Int. J. Miner. Process. **1997***,* 51, 171-181.
33. Sato, T.; Ruch, R. Stabilization of Colloidal Dispersions by Polymer Adsorption. **1980**, 155.
34. Hampton, A.; Nguyen, V. Nanobubbles and the Nanobubble Bridging Capillary Force. Adv. Colloid Interface Sci. **2010**, 154, 30-55.
35. Wang, L., Xu, Z. Physicochemical properties of heavy oil/water interfaces in the context of oil removal from sea water by froth flotation. In press, **2013.**
36. Adamson, W., Gast., P. Physical Chemistry of Surfaces. 6th ed; : Wiley publishing: New York, **1997**
37. Gu, G., Xu, Z., Nandakumar, K., Masliyah, J. Effects of Physical Environment on Induction Time of Air-Bitumen Attachment. Int. J. Miner. Process. **2003**, 69,235-250.
38. Kasongo, T., Zhou, Z., Xu, Z. Masliyah, J. Effect of Clays and Calcium Ions on Bitumen Extraction from Athabasca Oil Sands Using Flotation. J. Can. Chem. Eng. **2000**, 78,674-681.
39. Zhou, Z., Xu, Z., Masliyah, J. Factors Affecting the Recovery of Bitumen From Athabasca Oil Sands in Low Temperature Processes Using Floatation. In NSERC Chair Program, **2004**b.
40. Liu, J., Xu, Z., Masliyah, J. Interaction between Bitumen and Fines in Oil Sands Extraction System: Implication to Bitumen Recovery. J. Can. Chem. Eng. **2004**,

82,655-666.

41. Liu, J., Xu, Z., Masliyah, J. Role of Fine Clays in Bitumen Extraction from Oil Sands. J. AIChE. **2004**,50,1917-1927.
42. Liu, J., Xu, Z., Masliyah, J. Interaction Forces in Bitumen Extraction from Oil Sands. J. Colloid Interface Sci. **2005**, 287,507-520.
43. Liu, J., Xu, Z., Masliyah, J. Bitumen-Clay Interactions in Aqueous Media Studied by Zeta Potential Distribution Measurement. J. Colloid Interface Sci. **2002**, 252:409-418.
44. Wallace, D., Tipman, R. Fines/Water Interactions and Consequences of the Presence of Degraded Illite on Oil Sands Extractability. J. Can. Chem. Eng. **2004**,82,667-677.
45. Ding, X., Xu, Z., Masliyah, J. Effect of Illite Clay and Divalent Cations on Bitumen Recovery. J. Can. Chem. Eng. **2006**, 84,643-650.
46. Dang-Vu, T., Xu, Z., Masliyah, J. Effect of Solid Wettability on Processability of Oil Sands Ores. Energy Fuels **2009**, 23, 2628-2636.
47. Long, J., Xu, Z., Masliyah, J. Effect of Operating Temperature on Water-Based Oil Sands Processing. J. Can. Chem. Eng. **2007**, 85(5):726-738.
48. Ren, S., Dang-Vu,T., Zhao, H., Long, J., Xu, Z., Masliyah, J. Effect of Weathering on Surface Characteristics of Solids and Bitumen from Oil Sands. Energy Fuels **2009**, 23(1):334-341.
49. Ren, S., Dang-Vu,T., Zhao, H., Long, J., Xu, Z., Masliyah, J. Understanding Weathering of Oil Sands Ores by Atomic Force Microscopy. J. AIChE. **2009**,

55(12):3277-3285.

50. Primkulov, B.; Lin, F.; Xu, Z. Displacement Dynamics of Micro-droplets. In preparation.
51. Primkulov B.K. Bitumen Liberation Dynamics. MSc Thesis of University of Alberta. **2015**
52. Yoon, H., Yordan, L. Induction Time Measurement for the Quartz-Amine Flotation System. J. Colloid Interface Sci. **1991**, 141,374-383.
53. Hiemenz, C., Rajagopalan, R., Principles of Colloid and Surface Chemistry, 3 rd Edition, Marcel Dekker, New York, 1997.
54. Cai, B., Yang, J., Guo, T., Interfacial Tension of Hydrocarbon + Water/Brine Systems Under High Pressure, Journal of Chemical and Engineering Data, **1996**, 41, 493-496.
55. Hanly, G., Fornasiero, D., Ralston, J., Sedev, R. Electrostatics and Metal Oxide Wettability. J. phys. Chem. C **2011**, 115, 14914-14921.
56. Takamura, K. and Wallace, D. The Physical Chemistry of Hot Water Process. J. Can. Pet. Technol. **1988**, 27, 6.
57. Schramm, L., Smith, G., Stone, A. On the Processability of Mixtures of Oil Sands: AOSTRA J. Research, **1985**, 1, 147-161.